Electronic Supplementary Information for

Unveiling the formation mechanism of Pb_xPd_y intermetallic phases in solvothermal synthesis using *in situ* X-ray total scattering

Anders Bæk Borup,[a] Andreas Dueholm Bertelsen,[a] Magnus Kløve,[a] Rasmus Stubkjær Christensen,[a] Nils Lau Nyborg Broge,[a] Ann-Christin Dippel,[b] Mads Ry Vogel Jørgensen,[a,c] and Bo Brummerstedt Iversen[a*].

[a]Center for Integrated Materials Research, Department of Chemistry, Aarhus University, Langelandsgade 140, Aarhus 8000, Denmark
[b]Deutsches Elektronen-Synchrotron (DESY), Notkestraße 85, 22607 Hamburg, Germany
[c]MAX IV Laboratory, Lund University, 224 84 Lund, Sweden
*Corresponding author: bo@chem.au.dk

Table of content

S1: Comparison of Pb_3Pd_5 and Pb_9Pd_{13}.

In the following section, the problem with differentiating Pb_3Pd_5 and Pb_9Pd_{13} is described. Figure S1 compares the unit cells of Pb_3Pd_5 and Pb_9Pd_{13}, while Figure S2 compares their diffractograms and PDFs.

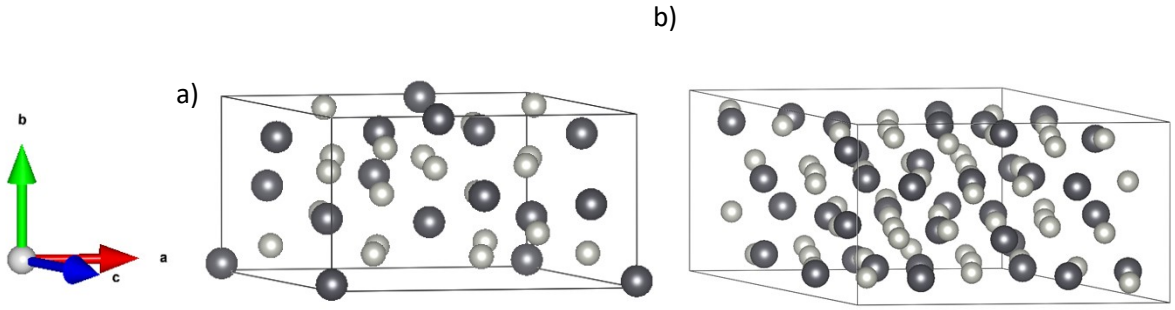

Figure S1. Comparison of the unit cells of a) Pb_3Pd_5 and b) Pb_9Pd_{13}. The figures are created using Vesta[1].

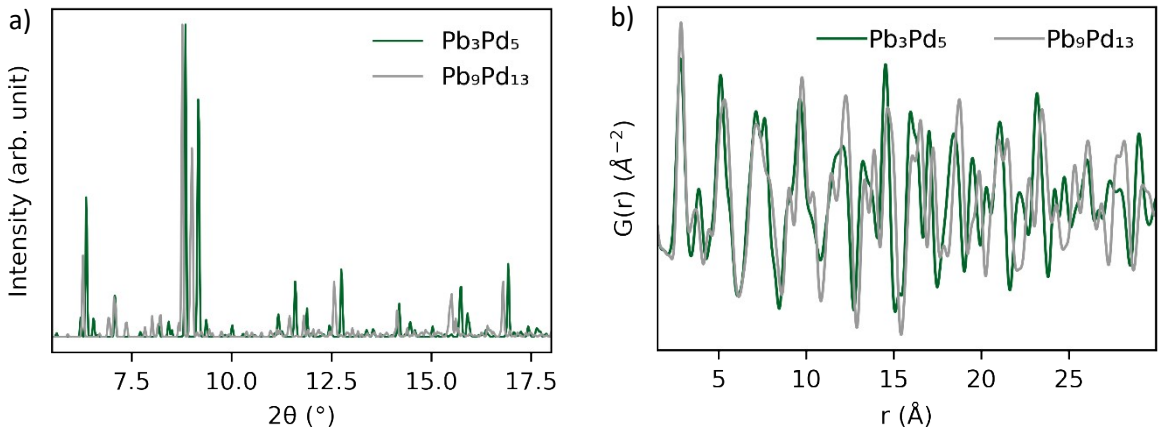

Figure S2. Simulation of a) diffractograms and b) PDFs for Pb_3Pd_5 and Pb_9Pd_{13}. The diffractograms are simulated using a wavelength of 0.35453 Å, while a Q_{max} of 13.1 Å^{-1} is used to simulate the PDF.

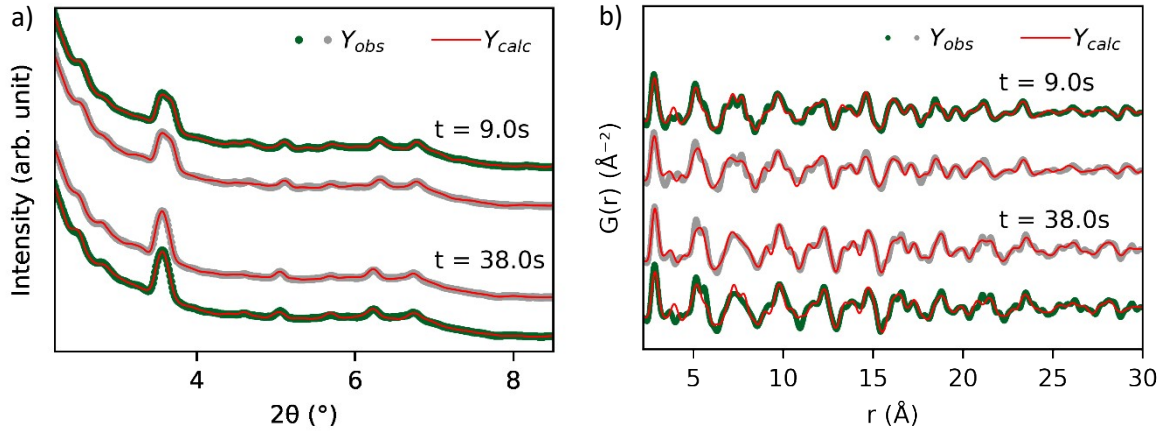

Figure S3. Comparing the a) PXRD and b) PDF fits obtained by using Pb_3Pd_5 and Pb_9Pd_{13} to the data at t = 9.0 s and t = 38.0 s for the 250 °C dataset. At each time, the top one is the fit for the phase believed to be present - Pb_3Pd_5 at t = 9.0 s and Pb_9Pd_{13} at t = 38.0 s.

Table S1: Comparing R_{wp} for fitting Pb_3Pd_5 and Pb_9Pd_{13} to the data at t=6.0 s and t=35.0 s for the 250 °C dataset. The rows marked in bold indicates the used phase.

t (s)	Phase	R_{wp} PXRD	R_{wp} PDF
9.0	**Pb_3Pd_5**	**0.70**	**29.06**
9.0	Pb_9Pd_{13}	0.91	37.19
38.0	**Pb_9Pd_{13}**	**0.60**	**27.00**
38.0	Pb_3Pd_5	0.97	37.41

Using the *in situ* data acquired at 250 °C, both phases have been fitted to the same frame. This is shown in Figure S3 with the corresponding R_{wp} values reported in Table S1. As is apparent from both the figure and the corresponding R_{wp} values, differentiating between the two phases in PXRD is difficult. However, PDF gives a clearer answer as using the wrong phase results in R_{wp} values, which are significantly higher. Visually, it is also possible to differentiate the PDFs, especially if considering the peaks between r = 5 Å and r = 10 Å.

However, in general it was not possible to describe the phase transitions by sequential PDF refinements. So, for the sequential PXRD refinements either Pb_3Pd_5 or Pb_9Pd_{13} is used to describe both phases. The sequential PXRD refinements reveal a change in unit cell volume for the Pb_3Pd_5/ Pb_9Pd_{13} phase, which is used to quantify the phase transition between the two phases. Figure S4 shows the development in unit cell parameters and unit cell lengths for Pb_3Pd_5/Pb_9Pd_{13} during the first 100 second of the *in situ* experiment at 250 °C. The gradual change in color from green to grey indicates the quantified phase transition. When the unit cell volume is at its lowest, we assume that only Pb_3Pd_5 is present, while we assume that only Pb_9Pd_{13} is present when the unit cell is at its maximum. Between these extrema, a linear relationship between the unit cell volume and the amount of Pb_3Pd_5/ Pb_9Pd_{13} is assumed.

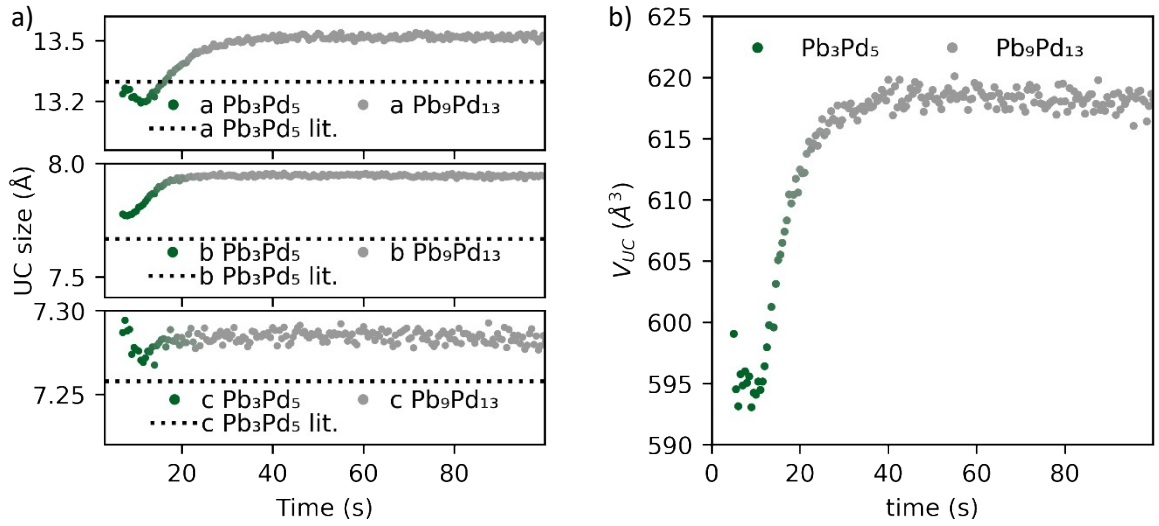

Figure S4. a) Development in unit cell parameters and b) unit cell volume for Pb_3Pd_5/Pb_9Pd_{13} obtained from Rietveld refinement during the first 100s for the *in situ* experiment at 250 °C. The dotted horizontal lines in Figure a) show the literature reported unit cell lengths for Pb_3Pd_5.[2]

S2: PDF generation

In this section, the PDF generation is quickly outlined. All PDFs are generated using the xPDFsuite.[3] For the *in situ* experiments, the temperature was constant during the relevant part of the experiments. Therefore, the same parameters and the same background have been used to generate the PDFs for the whole *in situ* experiment. An example of the generated PDFs is shown for each *in situ* experiment in Figures S5 - S9. Figures S10 and S11 shows the generation of the PDF for the two *ex situ* samples, where PDFs have been generated.

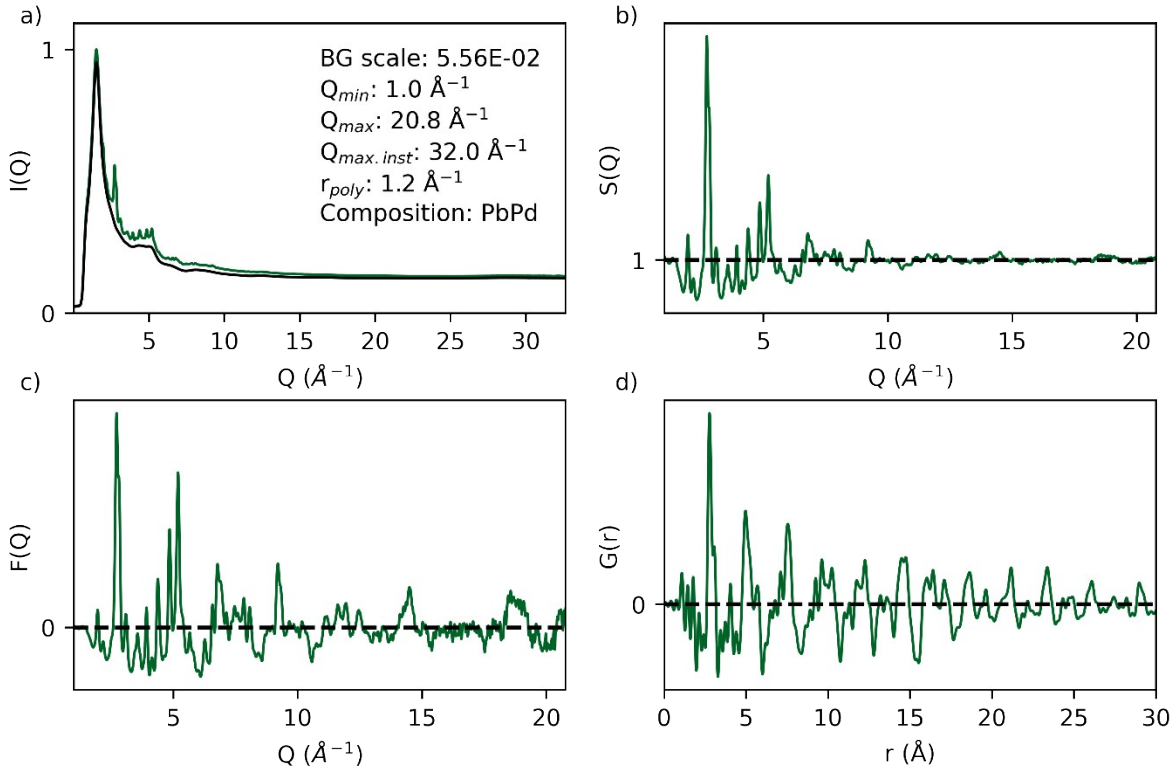

Figure S5. PDF generation for the *in situ* experiment at 150 °C with the frame at t = 1538.0 s used as an example. 20 detector frames have been summed to generate the PDFs. a) I(Q) and scaled ethylene glycol background used for subtraction, b) S(Q), c) F(Q), and d) G(r). The parameters used to generate the PDF in xPDFsuite are given in Figure a).

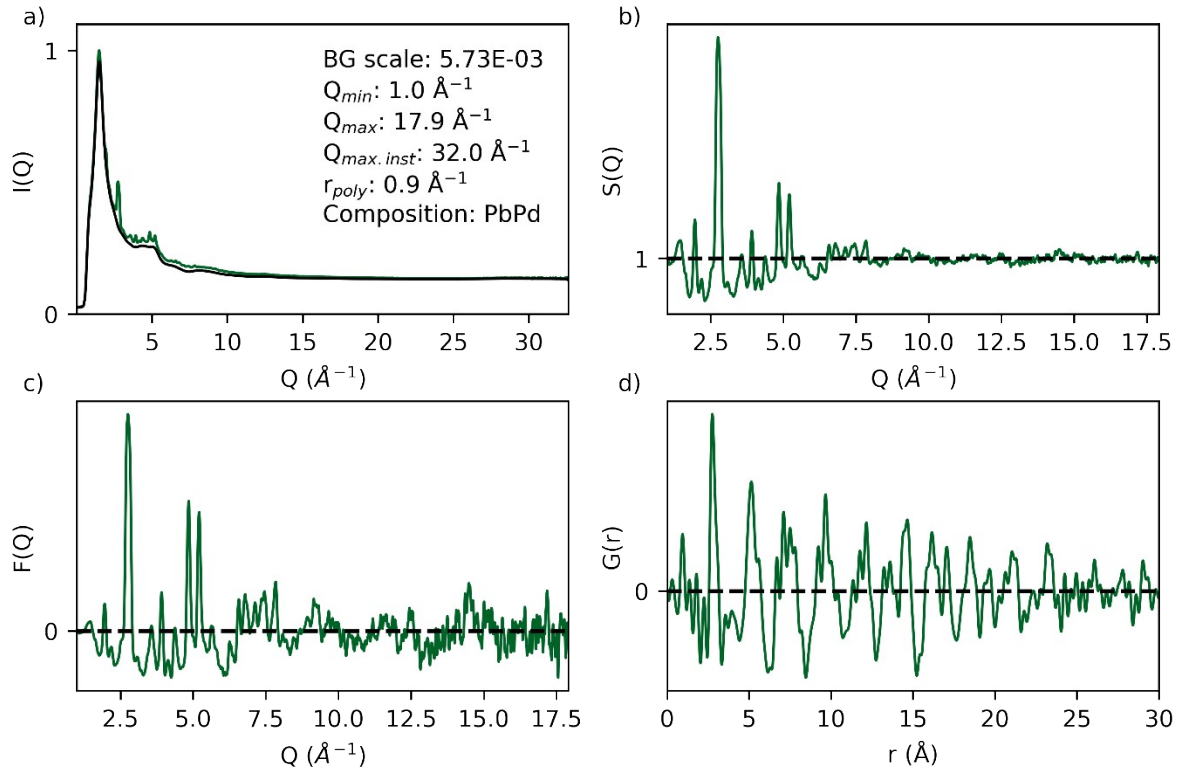

Figure S6. PDF generation for the *in situ* experiment at 200 °C with the frame at t = 93.0 s used as an example. 2 detector frames have been summed to generate the PDFs. a) I(Q) and scaled ethylene glycol background used for subtraction, b) S(Q), c) F(Q), and d) G(r). The parameters used to generate the PDF in xPDFsuite are given in Figure a).

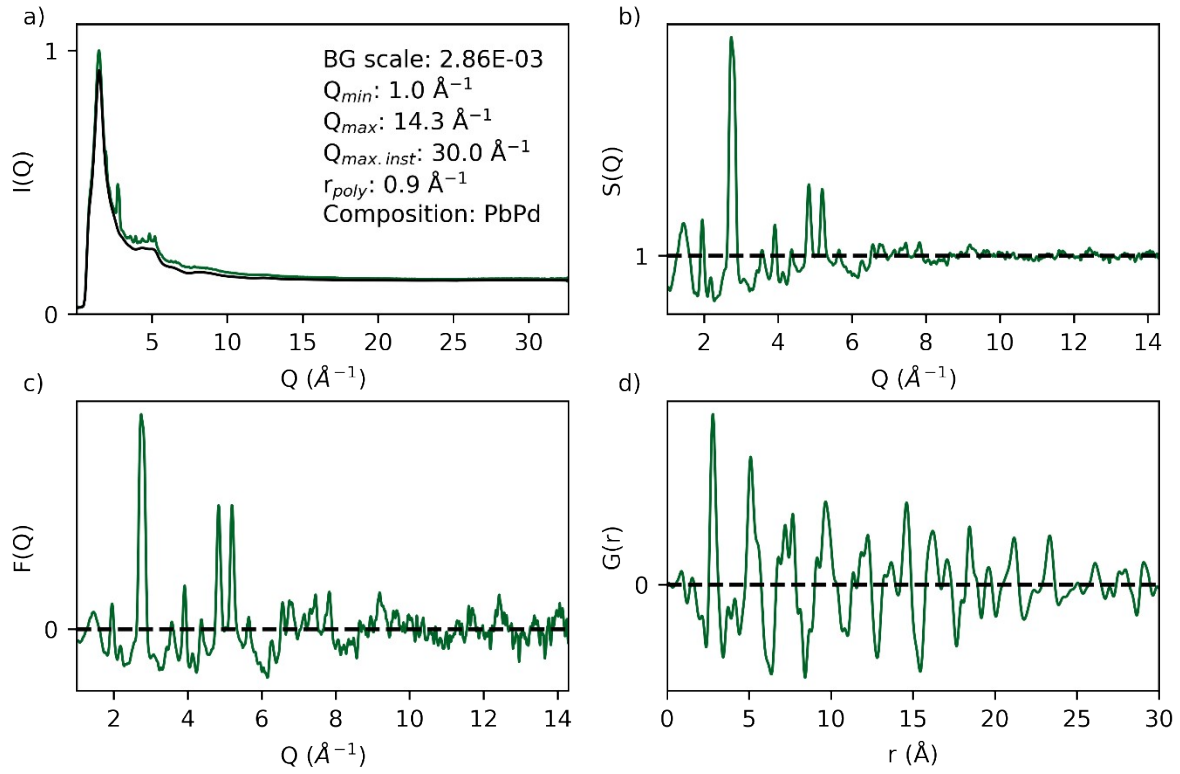

Figure S7. PDF generation for the *in situ* experiment at 250 °C with the frame at t = 9.0 s used as an example. a) I(Q) and scaled ethylene glycol background used for subtraction, b) S(Q), c) F(Q), and d) G(r). The parameters used to generate the PDF in xPDFsuite are given in Figure a).

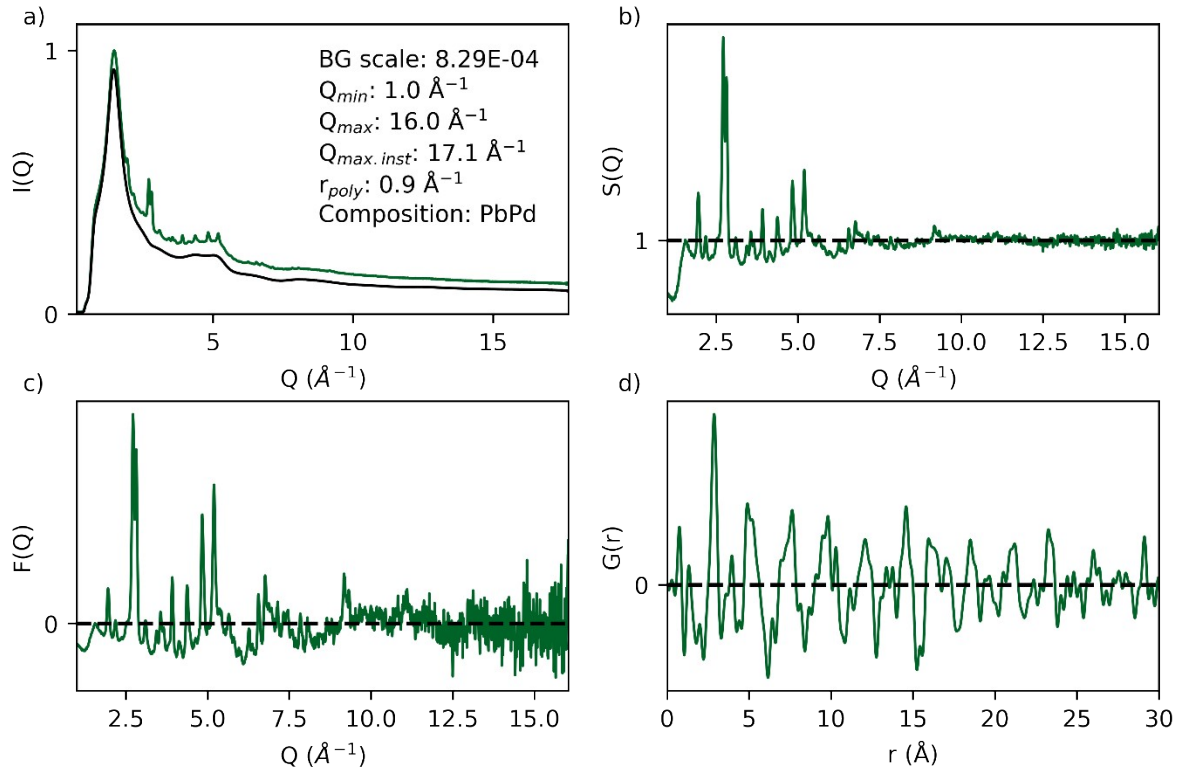

Figure S8. PDF generation for the *in situ* experiment at 300 °C with the frame at t = 6.0 s used as an example. a) I(Q) and scaled ethylene glycol background used for subtraction, b) S(Q), c) F(Q), and d) G(r). The parameters used to generate the PDF in xPDFsuite are given in Figure a).

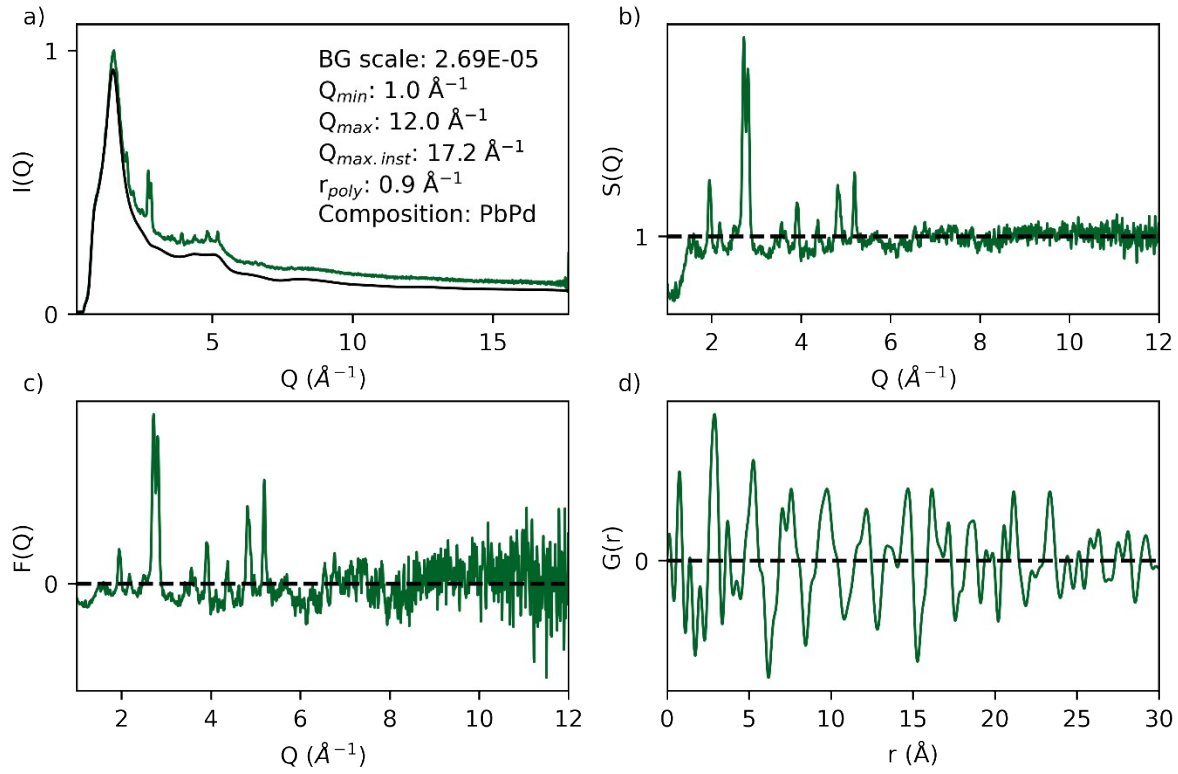

Figure S9. PDF generation for the *in situ* experiment at 350 °C with the frame at t = 5.0 s used as an example. a) I(Q) and scaled ethylene glycol background used for subtraction, b) S(Q), c) F(Q), and d) G(r). The parameters used to generate the PDF in xPDFsuite are given in Figure a).

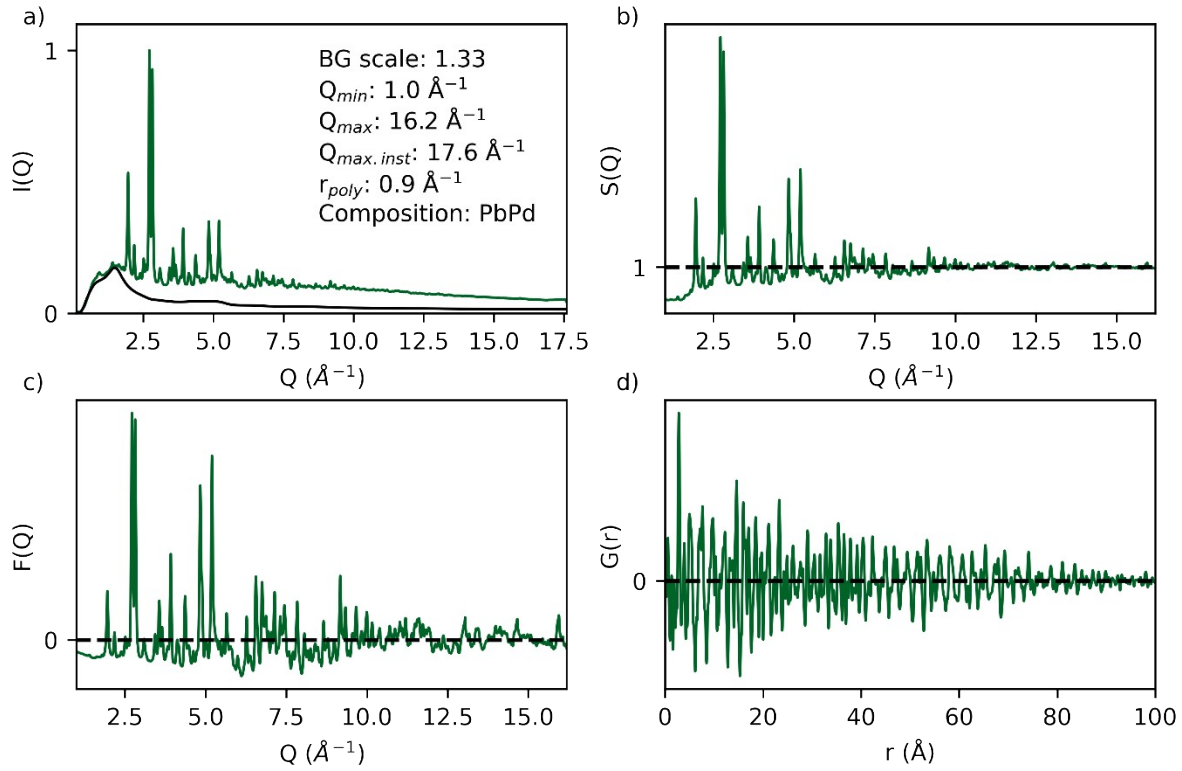

Figure S10. PDF generation for the *ex situ* experiment with a reaction temperature and time of 150 °C and 48 h. a) I(Q) and scaled quartz background used for subtraction, b) S(Q), c) F(Q) and d) G(r). The parameters used to generate the PDF in xPDFsuite are given in Figure a).

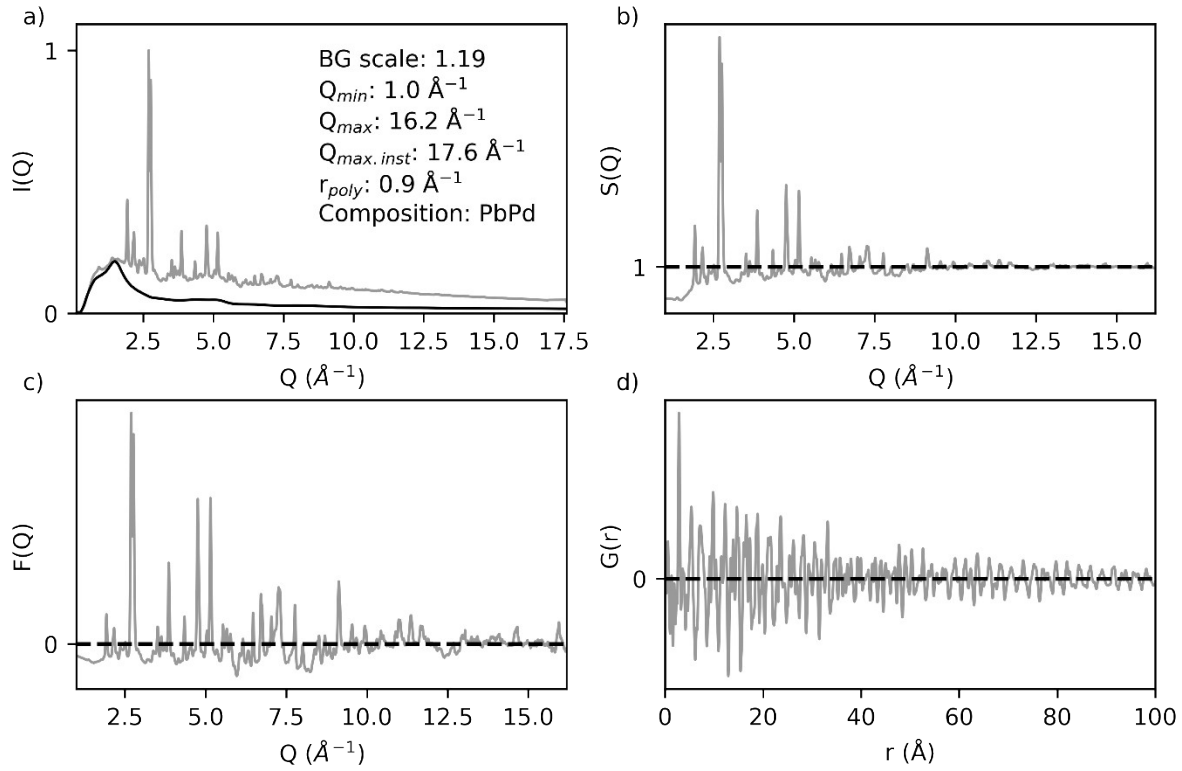

Figure S11. PDF generation for the *ex situ* experiment with a reaction temperature and time of 200 °C and 4 h. a) I(Q) and scaled quartz background used for subtraction, b) S(Q), c) F(Q) and d) G(r). The parameters used to generate the PDF in xPDFsuite are given in Figure a).

S3: In situ powder x-ray diffraction of the single-element precursors

Figure S12 shows the formation of Pb and Pd as a function of temperature. Pd nucleates around 100°C while Pb nucleates around 225°C.

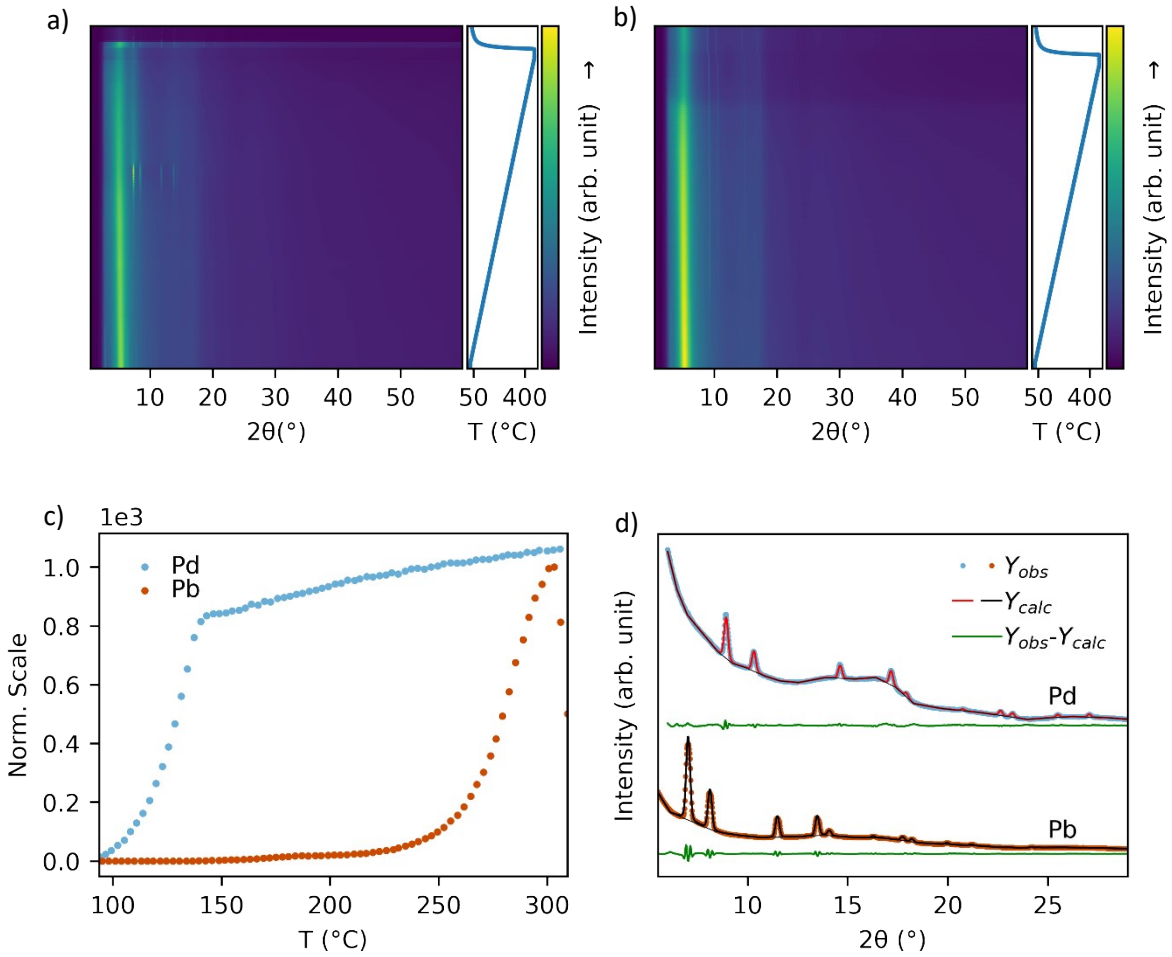

Figure S12. Data from the *in situ* experiment for a) $Pb(acac)_2$ and b) $Pd(acac)_2$ in ethylene glycol. c) The normalized scale factor from sequential Rietveld refinements as a function of temperature and d) the diffractograms at 300 °C with the corresponding fits.

S4: In situ powder x-ray diffraction for the solvothermal synthesis of Pb_xPd_y nanoparticles

In this section, the data for the *in situ* study of the formation of intermetallic Pb_xPd_y nanoparticles is shown. The temperature-calibration curve for the *in situ* solvothermal syntheses is shown, while fits of single frames used to identify the phases, the development in the scale factor, unit cell parameters and particle size are shown for the data collected at 150 °C, 200 °C, 300 °C and 350 °C. Some of the figures associated with the data collected at 250 °C are shown in the article, and therefore not shown here.

Temperature-calibration curve:

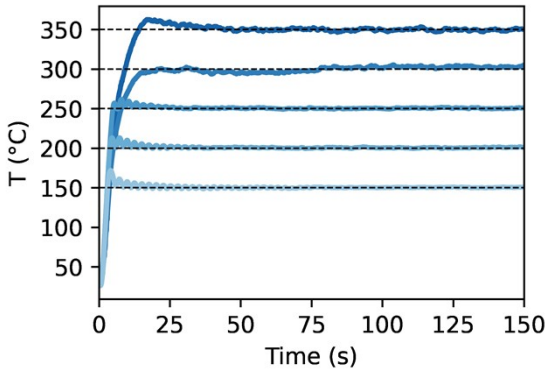

Figure S13. Temperature calibration curve for 150 °C °C, 200 °C, 250 °C, 300 °C and 350 °C. The 150 °C, 200 °C and 250 °C calibration curves are from the P21.1 beamtime, while 300 °C and 350 °C are from the DanMAX beamtime.

150°C:

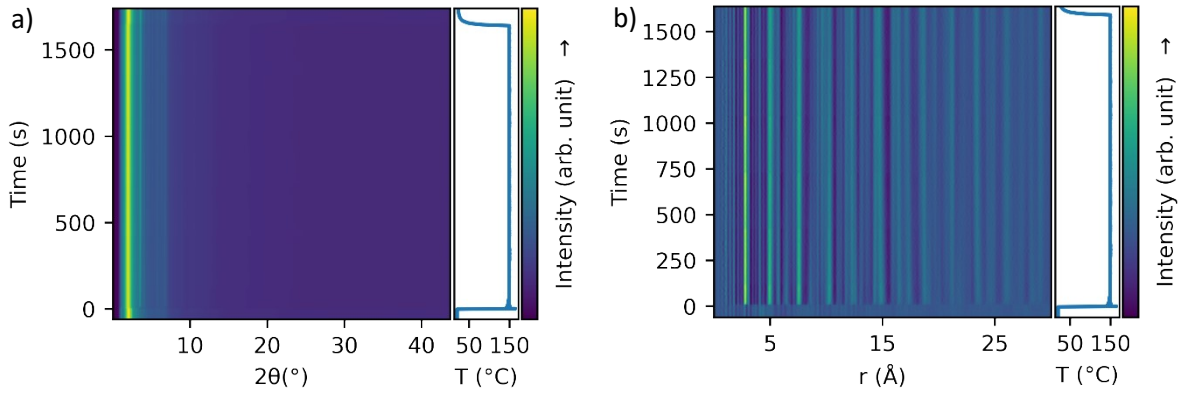

Figure S14. a) PXRD and b) PDF data from *in situ* experiment at 150 °C. For the PDF, a Q_{max} of 20.8 $Å^{-1}$ was used.

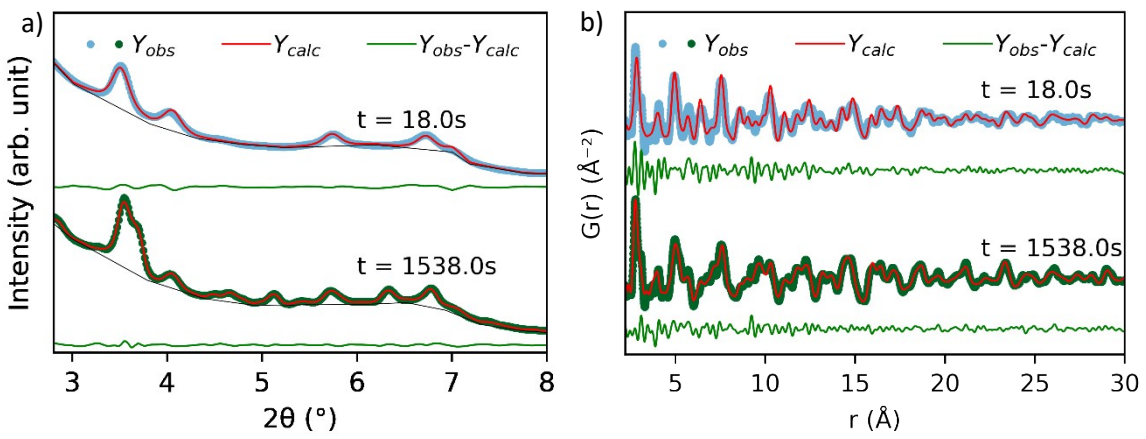

Figure S15. Fits of single frames. a) PXRD, b) PDF from *in situ* experiment at 150 °C. At 18.0 s Pd is fitted and at 1538.0 s Pd and Pb_3Pd_5 is fitted.

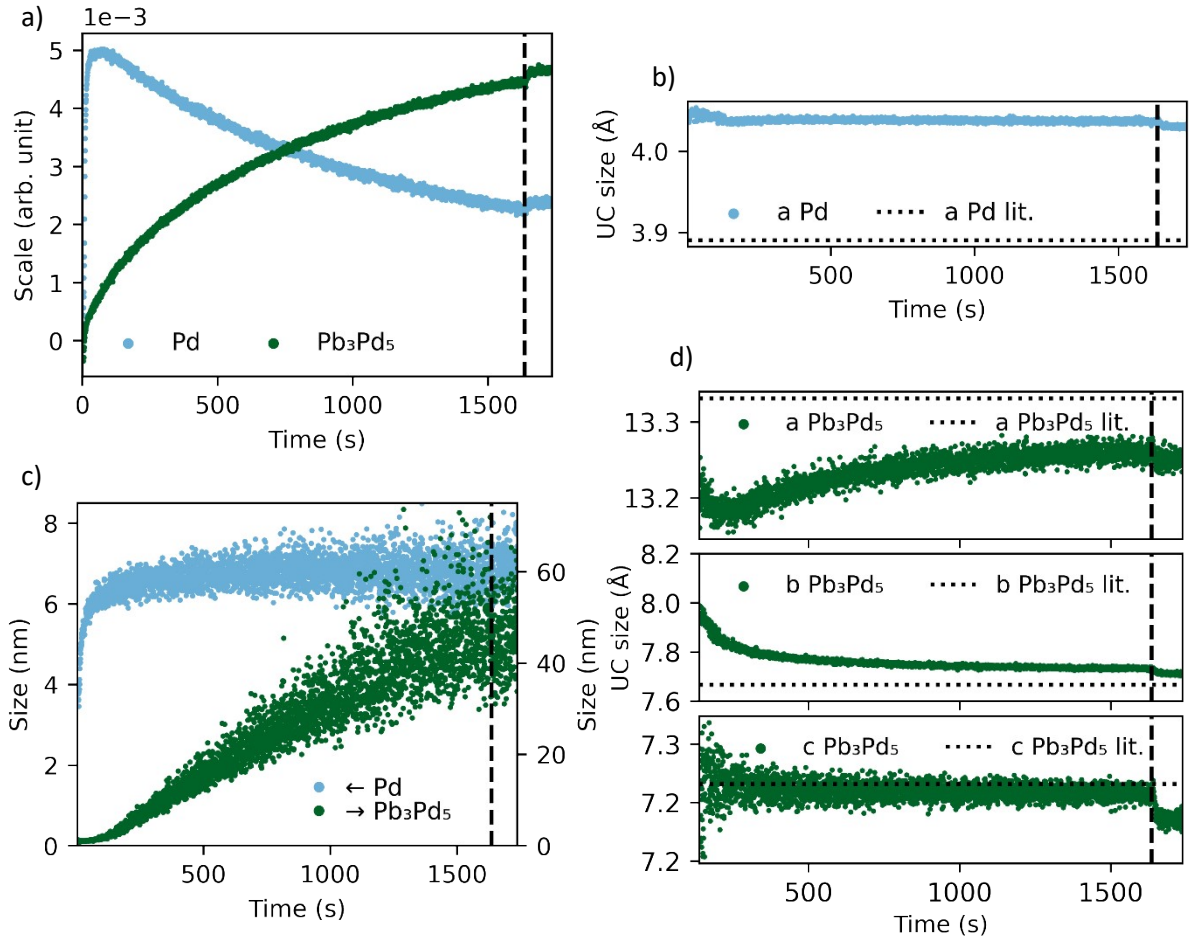

Figure S16. a) scale factor multiplied by unit cell volume and unit cell mass (SVM), b) and d) unit cell constants and c) particle size as a function of time from *in situ* experiment at 150 °C. The dotted vertical lines indicate cooling. The dotted horizontal line in the figure showing the development in unit cell parameters indicate the literature-tabulated values for the relevant Pb_xPd_y intermetallic phase.[2,4]

200°C:

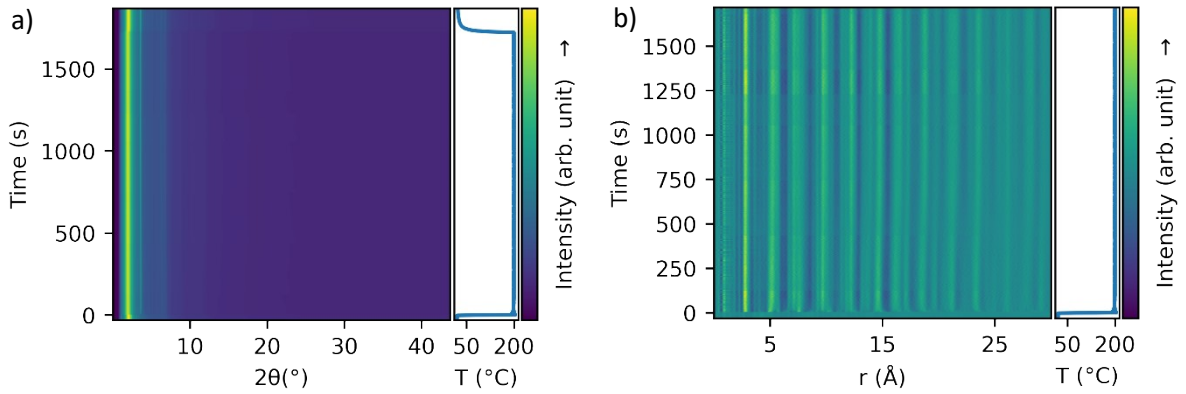

Figure S17. a) PXRD and b) PDF data from *in situ* experiment at 200 °C. For the PDF, a Q_{max} of 17.9 $Å^{-1}$ was used.

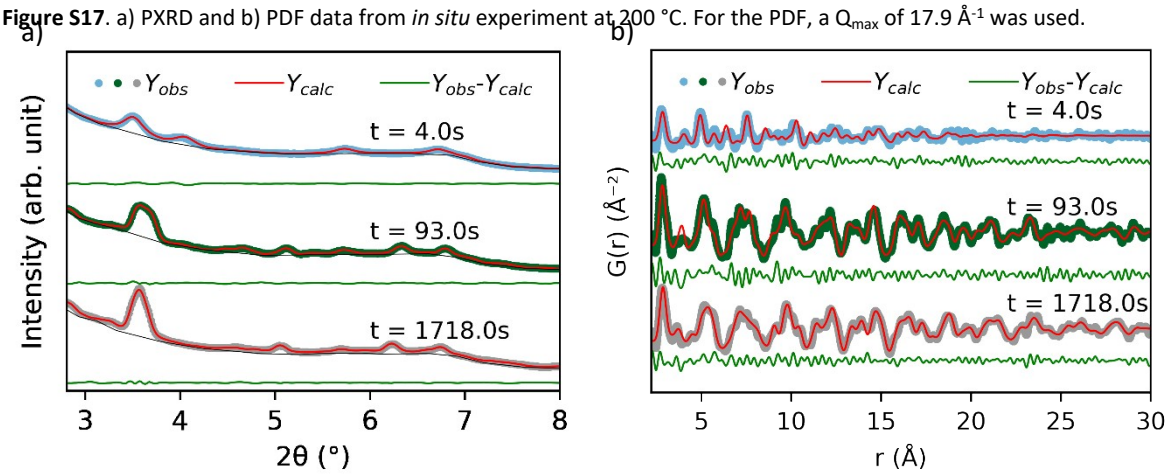

Figure S18. Fits of single frames. a) PXRD, b) PDF from *in situ* experiment at 200 °C. At 4.0 s Pd is fitted at 93.0 s Pb_3Pd_5 is fitted, and at 1718.0 s Pb_9Pd_{13} is fitted.

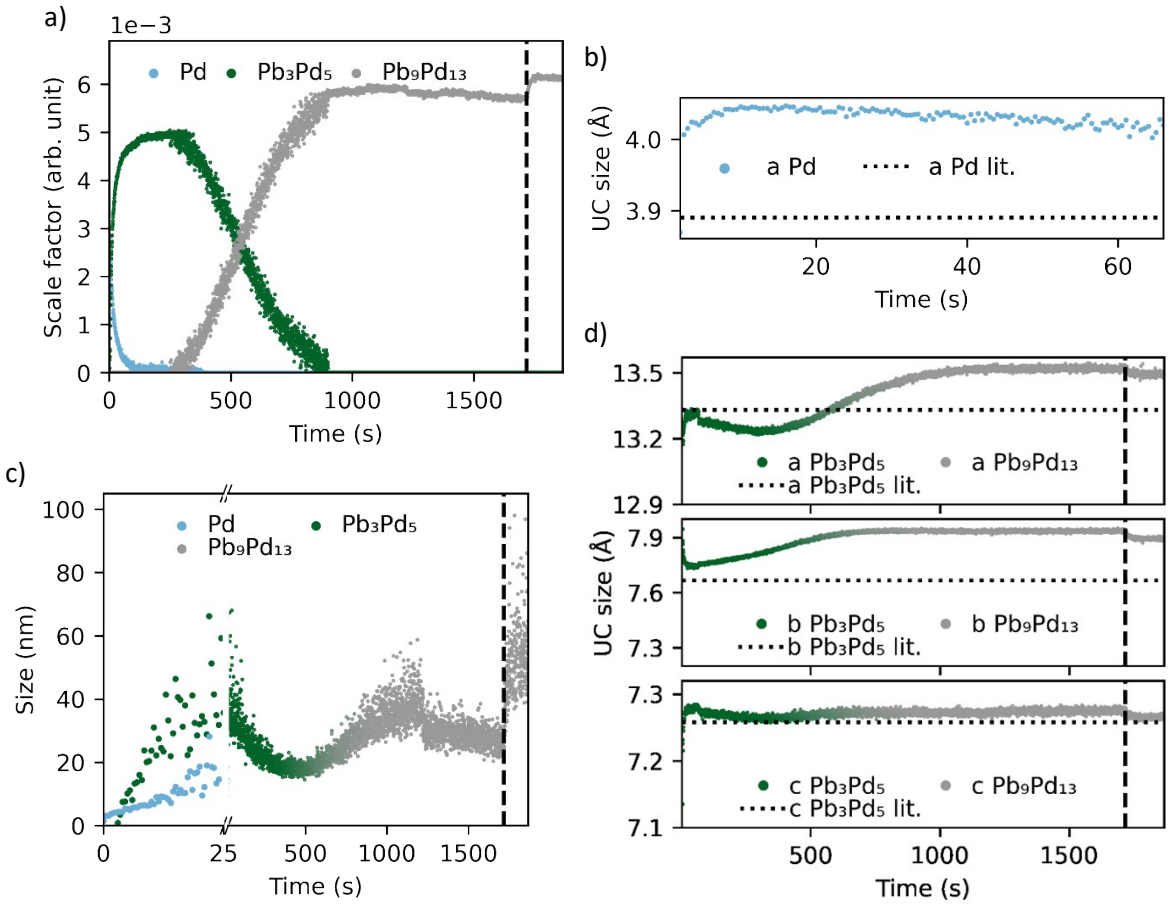

Figure S19. a) Scale factor multiplied by unit cell volume and weight (SVM), b) and d) unit cell constants and d) particle size as a function of time from *in situ* experiment at 200 °C.. The dotted vertical lines indicate cooling. The dotted horizontal line in the figures showing the development in unit cell constants indicates the literature tabulated values for the unit cell constants for the relevant Pb_xPd_y intermetallic phases.[2,4]

250°C:

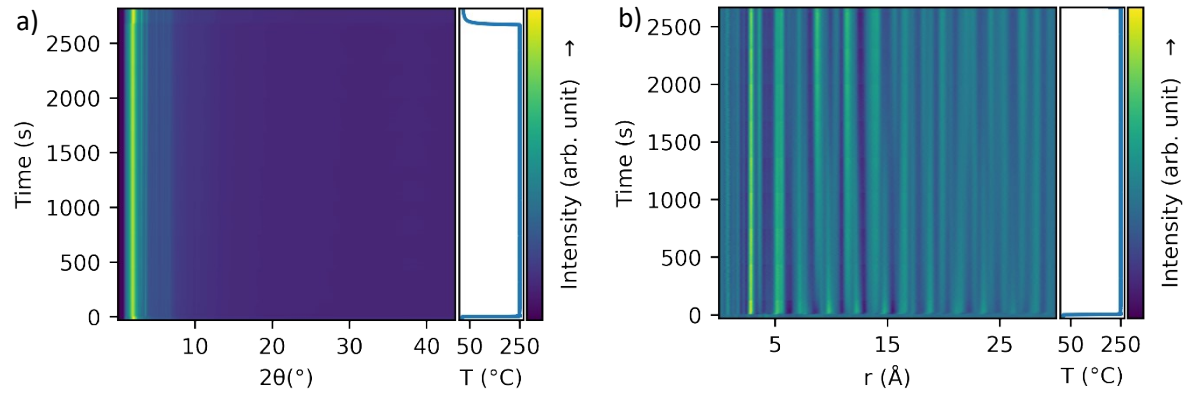

Figure S20. a) PXRD and b) PDF data from *in situ* experiment at 250 °C. For the PDF, a Q_{max} of 14.3 $Å^{-1}$ was used.

a)

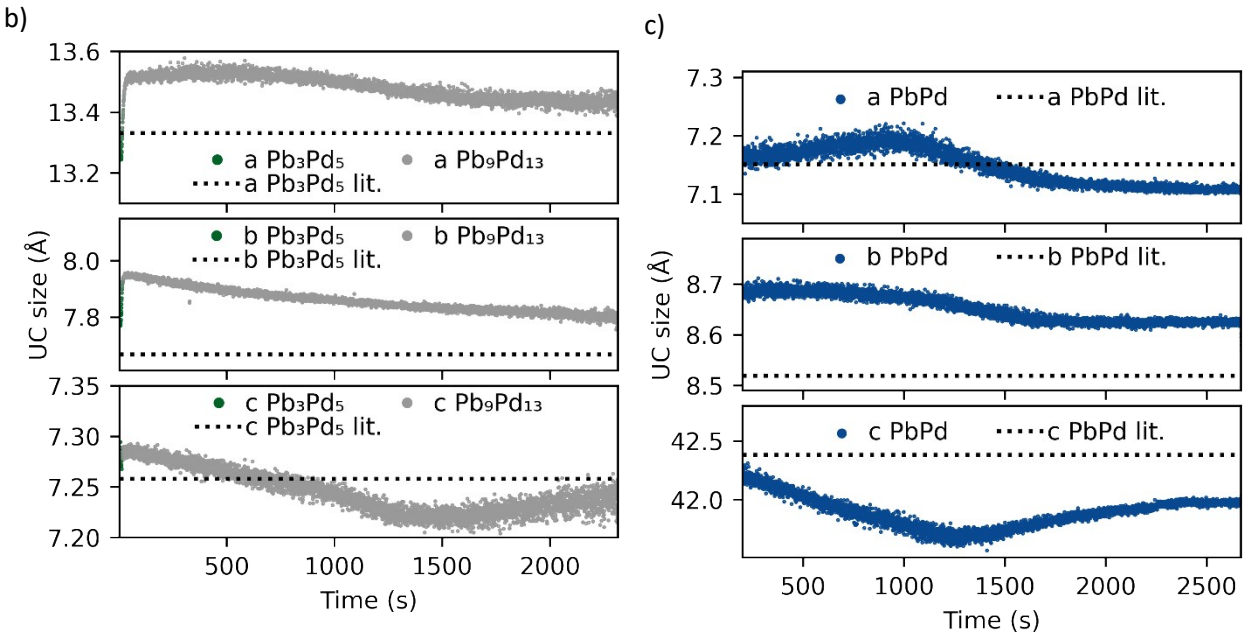

Figure S21. Unit cell parameters as a function of time from *in situ* experiment at 250 °C. The dotted horizontal line in the figures showing the development in unit cell constants indicates the literature tabulated values for the unit cell constants for the relevant Pb_xPd_y intermetallic phases. [2,4,6]

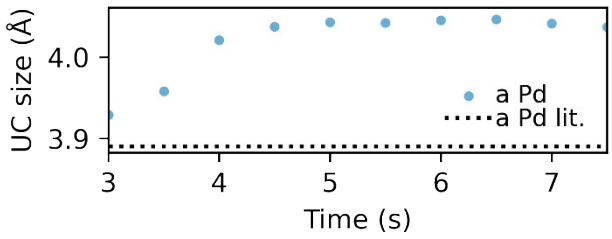

300°C:

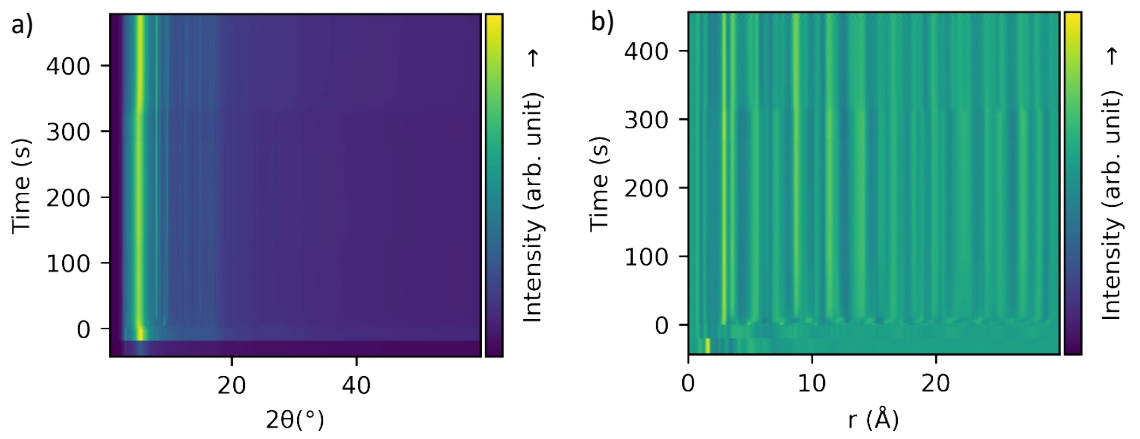

Figure S22. a) PXRD and b) PDF data from *in situ* experiment at 300 °C. For the PDF, a Q_{max} of 16.0 $Å^{-1}$ was used. Due to technical errors, temperature data is not available for this experiment.

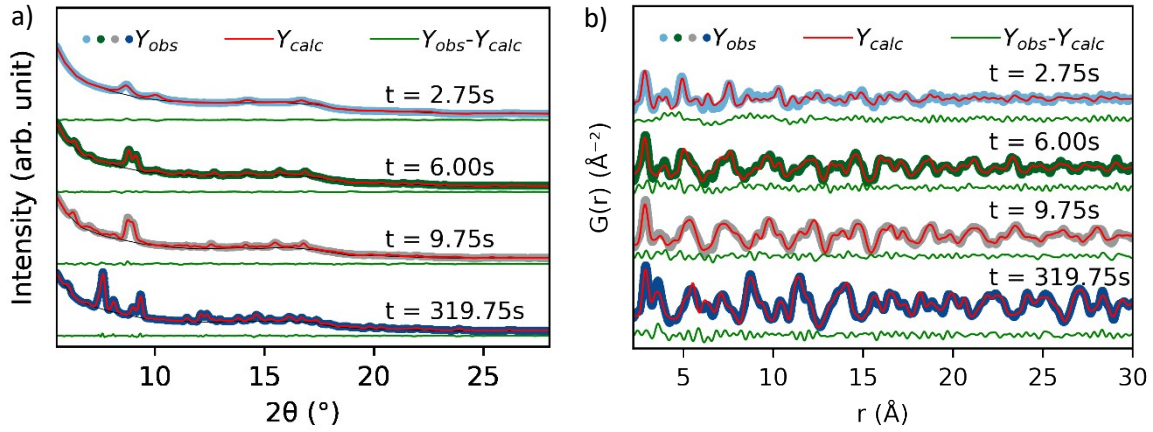

Figure S23. Fits of single frames. a) PXRD, b) PDF from *in situ* experiment at 300 °C. At 2.75 s Pd is fitted (Pb_3Pd_5 is also fitted in the PDF), at 6.00 s Pd and Pb_3Pd_5 is fitted, at 9.75 s Pb_9Pd_{13} is fitted, while PbPd and Pb_2Pd is fitted at 319.75 s.

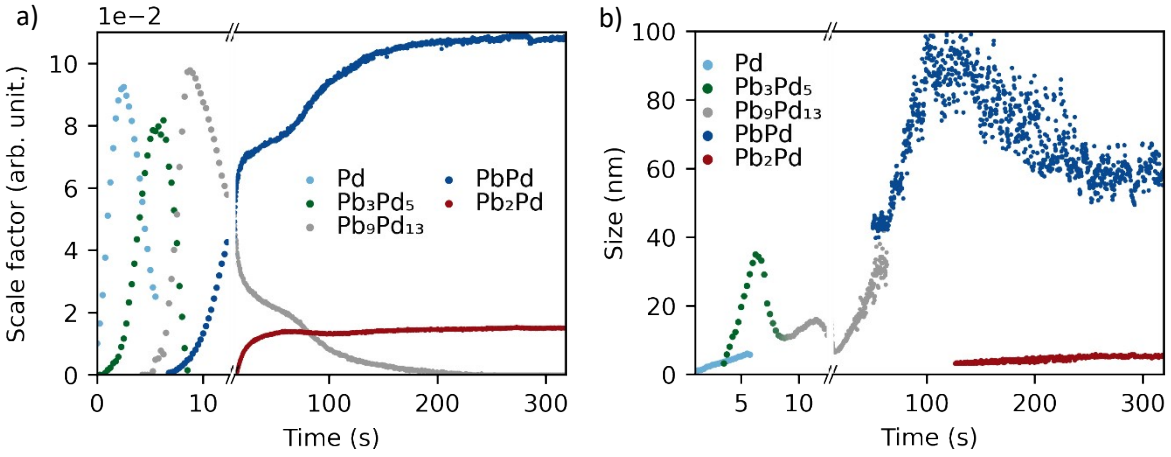

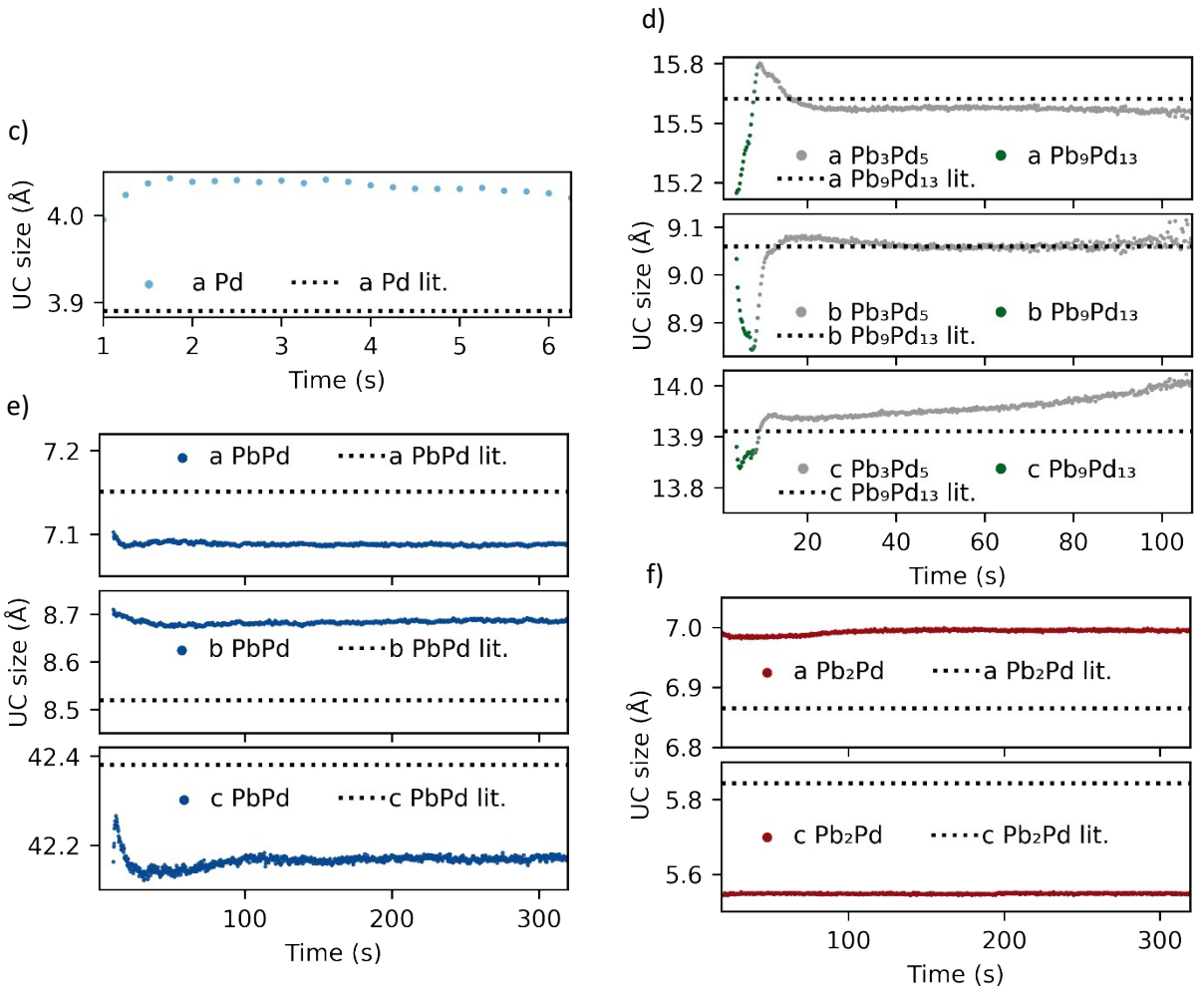

Figure S24. a) Scale factor multiplied by unit cell volume and weight (SVM), b) particle size, and c-f) unit cell parameters as a function of time from *in situ* experiment at 300 °C. For the figures showing the development in unit cell parameters, the horizontal dotted line indicates the literature tabulated values for the relevant Pb_xPd_y phases.[4-7]

350°C:

Due to a data acquisition error, a gap of approx. 8 minutes appears in the data.

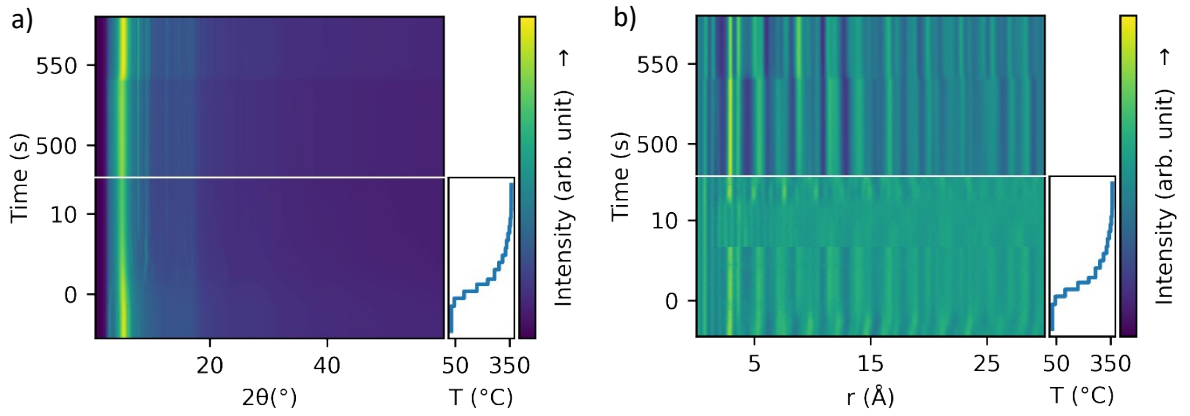

Figure S25. a) PXRD and b) PDF data from *in situ* experiment at 350 °C. For the PDF, a Q_{max} of 12.0 $Å^{-1}$ was used before the 8 minute gap, while a Q_{max} of 12.8 $Å^{-1}$ was used after. Due to technical errors, temperature data is not available for the second half of this experiment.

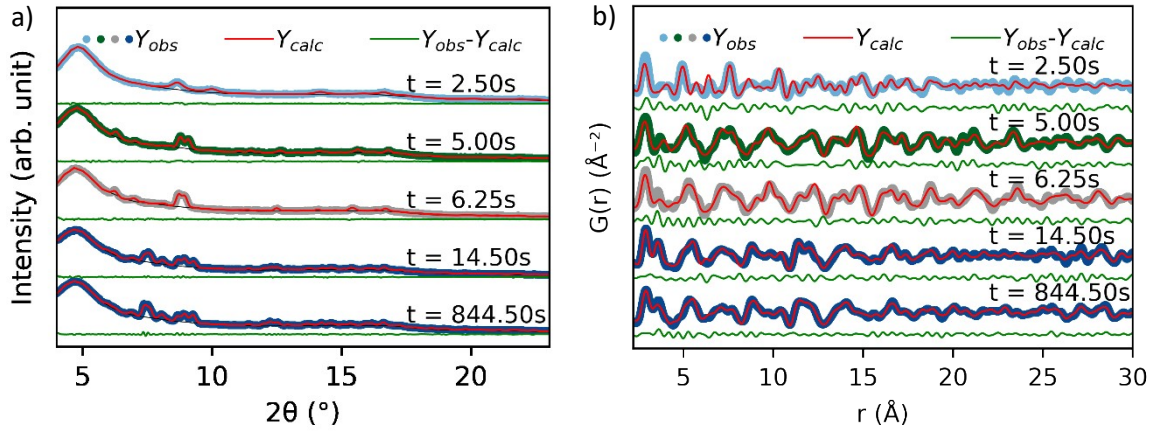

Figure S26. Fits of single frames. a) PXRD, b) PDF from *in situ* experiment at 350 °C. At 2.50 s Pd is fitted, at 5.00 s Pb_3Pd_5 is fitted, at 6.25 s Pb_9Pd_{13} is fitted, while Pb_9Pd_{13}, PbPd, and Pb_2Pd is fitted at 14.50 s and 844.50 s.

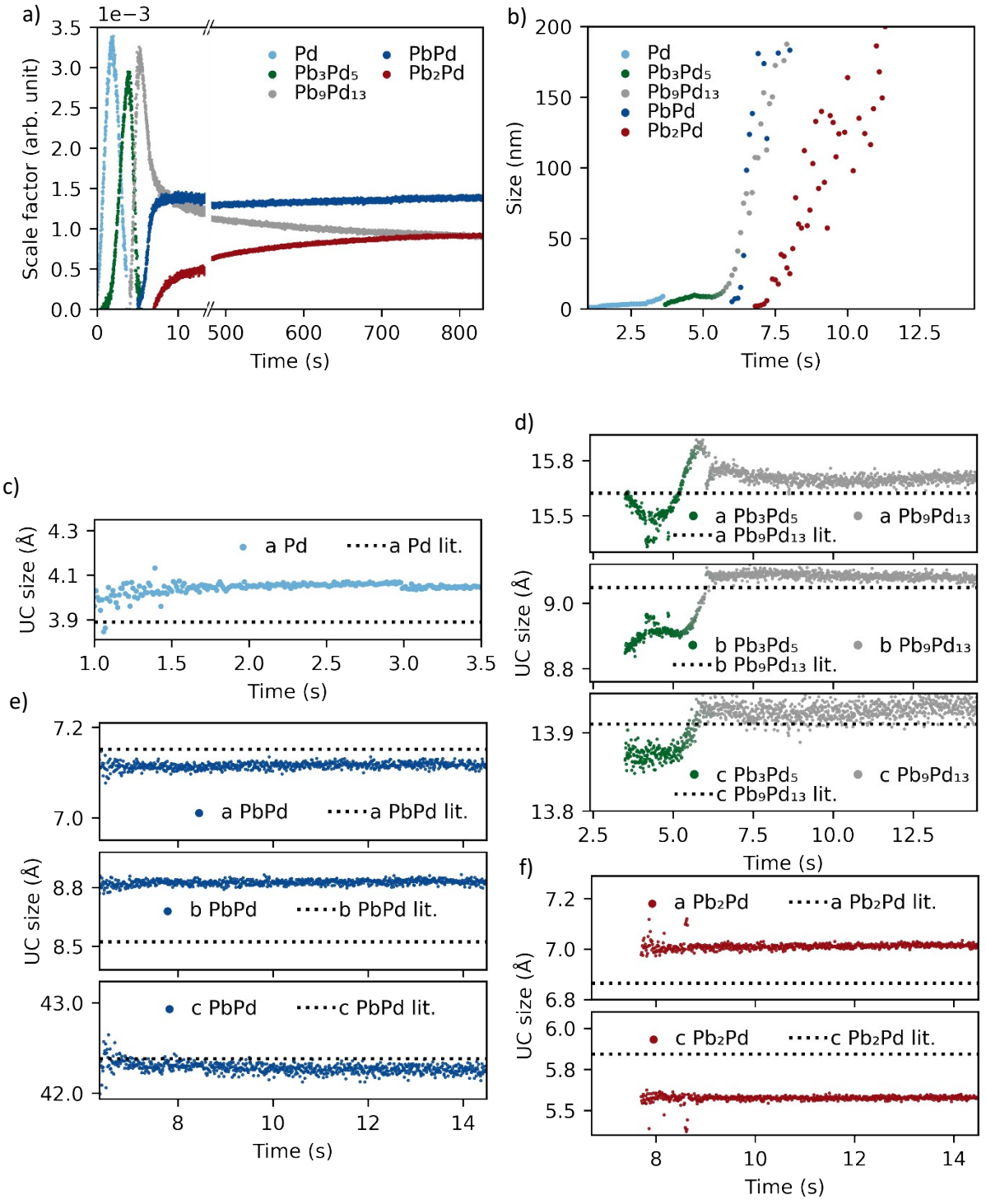

Figure S27. a) Scale factor multiplied by unit cell volume and weight (SVM), b) particle size, and c-f) unit cell parameters as a function of time from *in situ* experiment at 350 °C. The scale factor has been scaled to account for the different exposure times during the first and second part of the experiment. For the figures showing the development in unit cell parameters, the horizontal dotted line indicates the literature tabulated values for the relevant Pb_xPd_y phases.[4-7]

S5: In situ powder X-ray diffraction for the solvothermal seeded synthesis of Pb_xPd_y nanoparticles

To support the mechanism, an experiment using Pd nanoparticles and $Pb(acac)_2$ as the precursors and a reaction temperature of 250 °C was performed. The experimental details are included in the experimental section of the article. Before the sequential refinement, 5 data frames were summed, resulting in an effective exposure of 0.5 s.

The data is shown in Figure S28, with the figures also contain refinements of single frame at t = 11.5 s, t = 151.0 s, and t = 1667.0 s respectively. The single frame refinements clearly show that in the beginning Pd nanoparticles are present, whereafter Pb_xPd_y intermetallic phases are formed. Since the only Pd precursor present is Pd nanoparticles, the formation of Pb_xPd_y intermetallic phases must be a result of Pb diffusion into the Pd-rich structure, confirming the diffusion step of the mechanism.

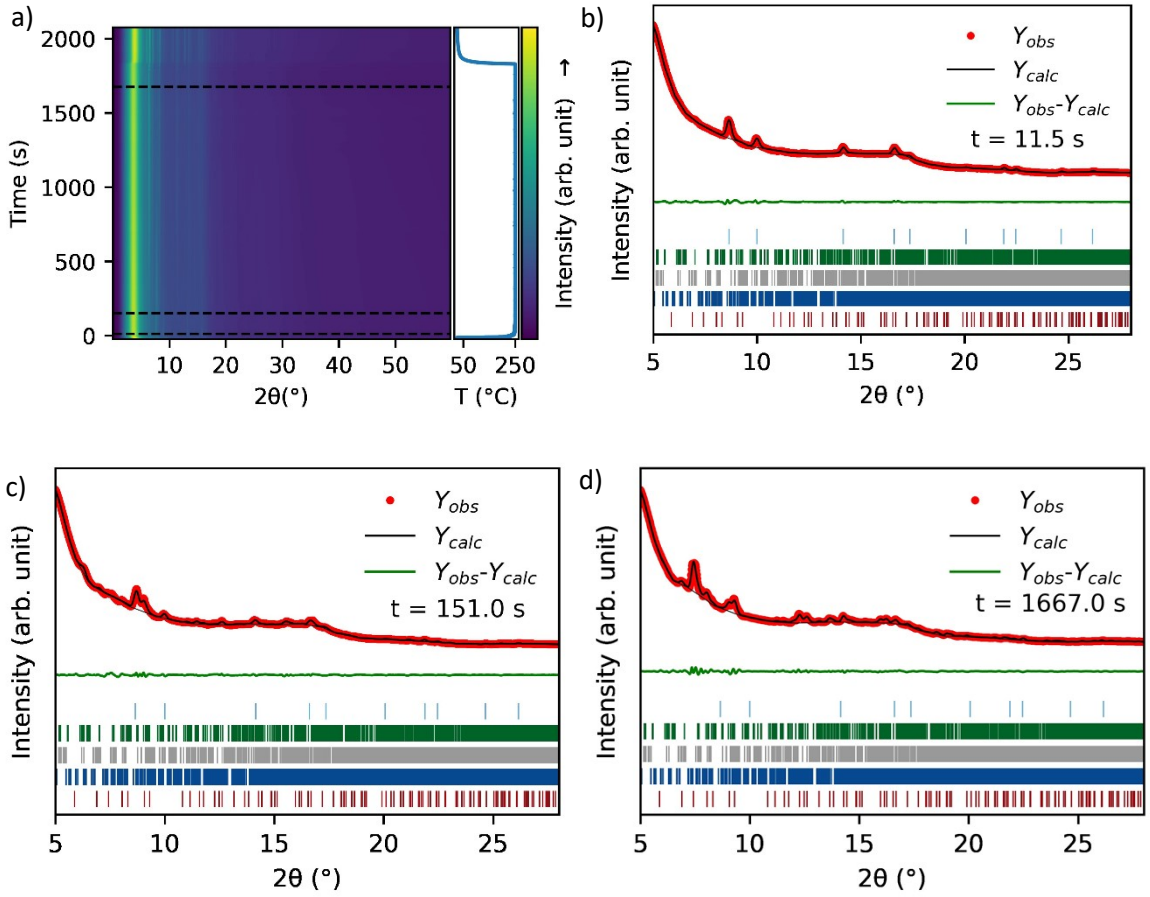

Figure S28: a) PXRD data from the seeded *in situ* experiment at 250 °C. b) single diffractogram at t = 11.5 s. Pd has been used to Rietveld refine the data. c) single diffractogram at t = 151.0 s. Pd and Pb_3Pd_5 has been used to Rietveld refine the data. d) single diffratogram at t = 1667.0 s. PbPd and Pb_2Pd has been shown to Rietveld refine the data. At b), c), and d), the expected reflections for Pd (light blue), Pb_3Pd_5 (dark green), Pb_9Pd_{13} (grey), PbPd (dark blue), and Pb_2Pd (dark red) are shown.

S6: Ex situ autoclave experiments

In this section, the results from all the conducted *ex situ* autoclave experiments are covered. Table S2 summarizes the results from the Rietveld refinements, while Figures S30-S38 visually compare the fit with the measured data.

Table S2. Results from Rietveld refinements. A dash instead of the size indicates that the particles no longer are nanosized and the size are therefore not possible to model.

T (°C)	t (hours)	Phase	Wt%	Diameter (nm)	R_{wp} (%)
150	4	Pd	78.9(3)	9.6(3)	3.08
		Pb_3Pd_5	21.1(3)	16.8(15)	
150	24	Pd	21.9(3)	39(3)	3.53
		Pb_3Pd_5	78.1(3)	52(2)	
150	48	Pd	6.4(4)	38(13)	4.67
		Pb_3Pd_5	93.6(4)	44(2)	
200	4	Pb_9Pd_{13}	94.1(3)	44.2(13)	2.82
		PbPd	5.9(3)	-	
240	4	Pd	3.9(3)	-	3.63
		Pb_3Pd_5	25.5(6)	39(7)	
		Pb_9Pd_{13}	54.6(6)	24.4(14)	
		PbPd	16.1(3)	37(6)	
300	4	Pd	5.0(2)	56(10)	3.66
		Pb_3Pd_5	24.4(3)	52(3)	
		Pb_9Pd_{13}	33.3(3)	48(3)	
		PbPd	18.2(2)	$17(4)\cdot10^1$	
		Pb_2Pd	13.1(2)	178(11)	
		PbO	5.9(4)	4.9(3)	
350	4	Pd	4.2(2)	32(4)	4.36
		Pb_9Pd_{13}	20.6(2)	21.1(7)	
		PbPd	72.8(2)	198(15)	
		Pb_2Pd	2.39(15)	$6(2)\cdot10^1$	

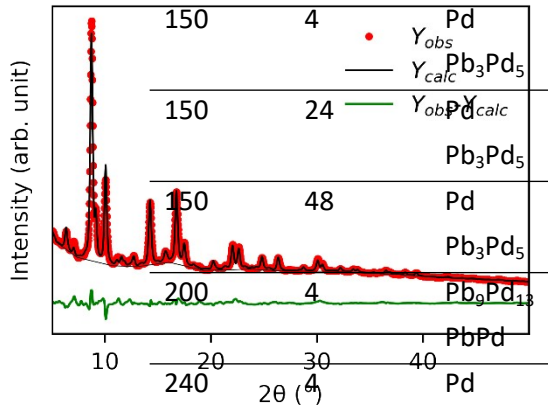

Figure S29: PXRD, synthesis at 150 °C and 4 h.

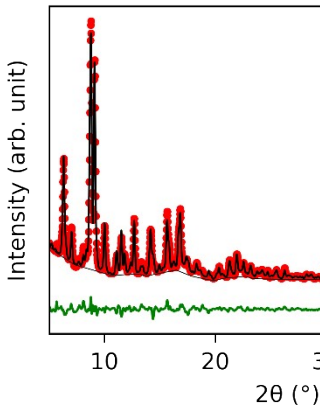

Figure S30: PXRD, synthesis at 150 °C and 24 h

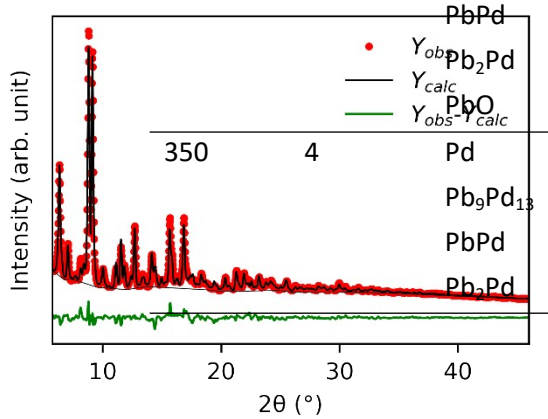

Figure S31: PXRD, synthesis at 150 °C and 48 h.

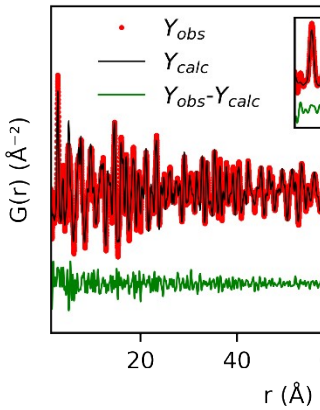

Figure S32: PDF, synthesis at 150 °C and 48 h. A Q_{max} of 16.2 Å^{-1} was used.

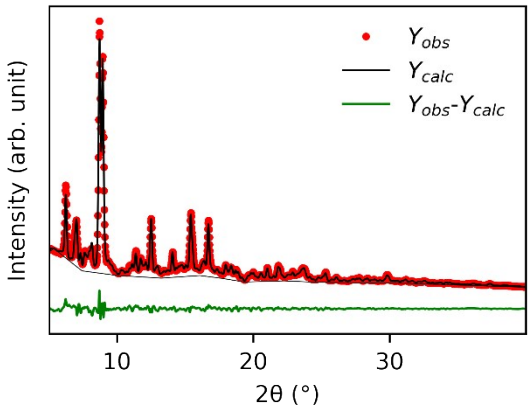

Figure S33: PXRD, synthesis at 200 °C and 4 h.

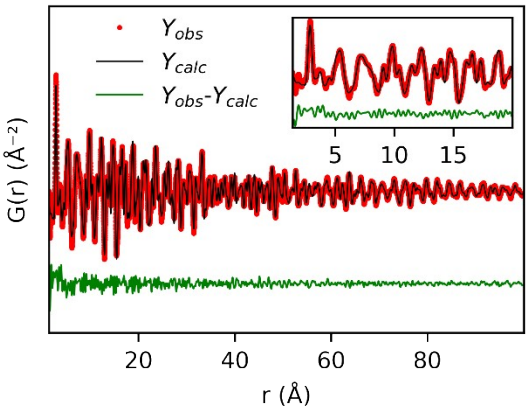

Figure S34: PDF, synthesis at 200 °C and 4 h. A Q_{max} of 16.2 Å^{-1} was used.

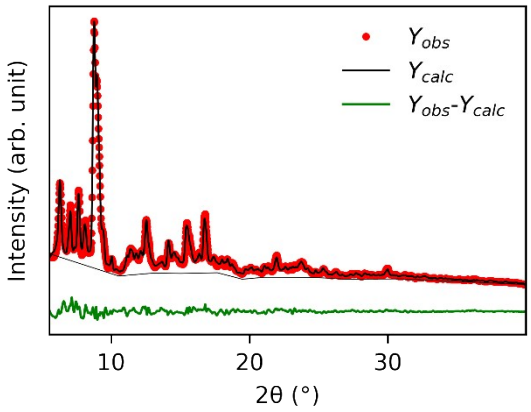

Figure S35: PXRD, synthesis at 250 °C and 4 h.

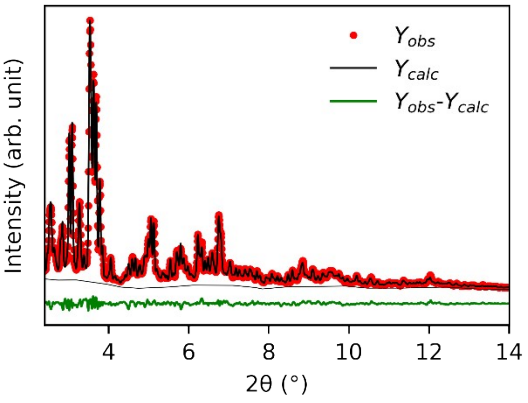

Figure S36: PXRD, synthesis at 300 °C and 4 h.

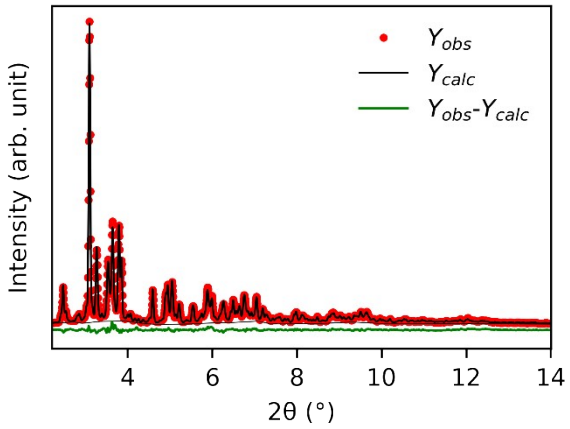

Figure S37: PXRD, synthesis at 350 °C and 4 h.

S7: Additional STEM images.

Figure S38 and S39 shows additional STEM images of the synthesize Pb_3Pd_5. As is apparent from Figure S38, the size of 44(2) nm obtained from PXRD seems reasonable. In some places small particles were apparent. In Figure S39 a large region with these small particles is found, with the EDX-spectrum revealing the particles as Pb-particles.

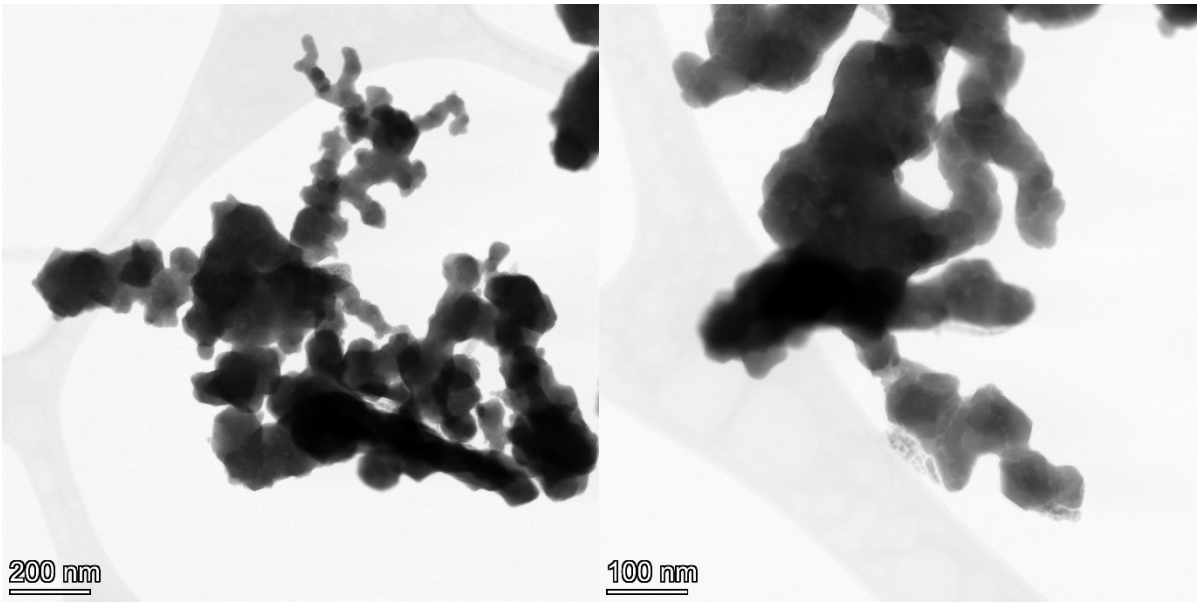

Figure S38. Bright-field STEM images of Pb_3Pd_5 from the synthesis at 150 °C and 48 h.

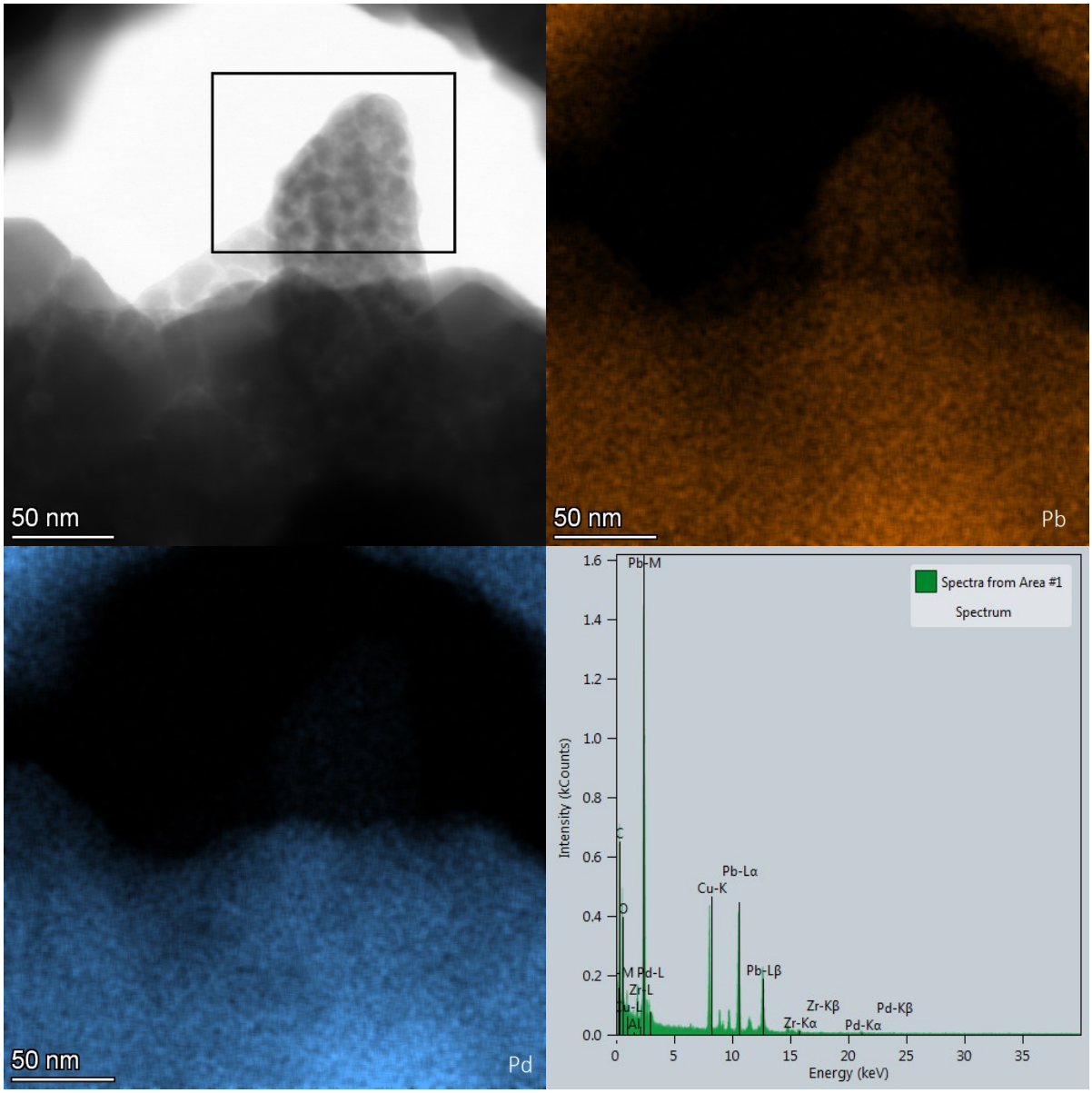

Figure S39: STEM-EDS images of Pb_3Pd_5 from the synthesis at 150 °C and 48 h. The rectangle indicates the area, where the EDS graph applies.

S8: Results from Rietveld refinement of Pd nanoparticles

The Pd nanoparticles used as a reference for the electrochemical measurements are characterized by a Rietveld refinement. The refined model compared with the acquired data is shown in Figure S40. During the refinement, an anisotropic size distribution was used. The model indicates (111) as the preferred growing direction and a particle size of 3.09(4) nm x 3.09(4) nm x 3.25(3) nm.

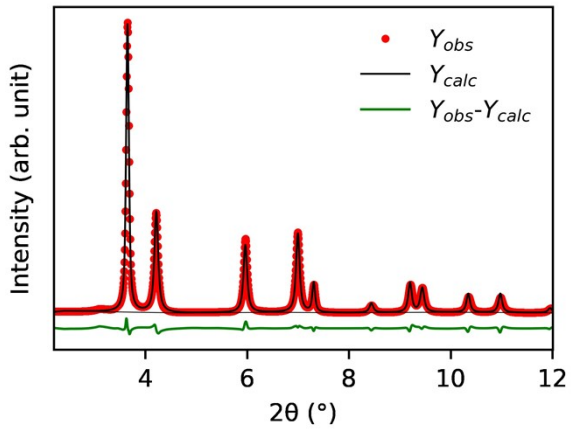

Figure S40: PXRD, Pd nanoparticles used as reference for HER. R_{wp} = 6.95%.

S9: SEM images and PXRD of electrodes before and after HER.

The Pb and $PbPd_x$ thin films before and after the stability test towards HER are characterized by SEM and grazing incidence PXRD. Figure S41 - S43 shows the SEM images of Pd, Pb_3Pd_5, and Pb_9Pd_{13} thin films before and after performing the electrochemical experiments, while Figure S44 shows the corresponding diffractograms. No apparent changes are observed in the SEM images and PXRD. The spectra shown in the SEM figures reveal the elemental composition and the amount of each element. Besides Pb and Pd, carbon, and fluorine are detected, but omitted from the results in the following figures. The electrodes are made from glassy carbon, giving rise to the carbon signal, while they are surrounded by Teflon. Furthermore, we add Nafion, whereby the fluorine signal can be explained. The edges the program uses to identify the elements are listed in Table S3.

Table S3: The elements found in the SEM-EDX pictures and their emission energy.

Element	Energy (keV)
C	0.277
F	0.677
Pd	0.284
Pd	2.503
Pd	2.660
Pd	2.839
Pd	2.990
Pd	3.553
Pb	0.276
Pb	0.293
Pb	1.823
Pb	2.345
Pb	2.663
Pb	9.185

Pb	10.552
Pb	11.349
Pb	12.614
Pb	12.623
Pb	14.765
Pb	15.101

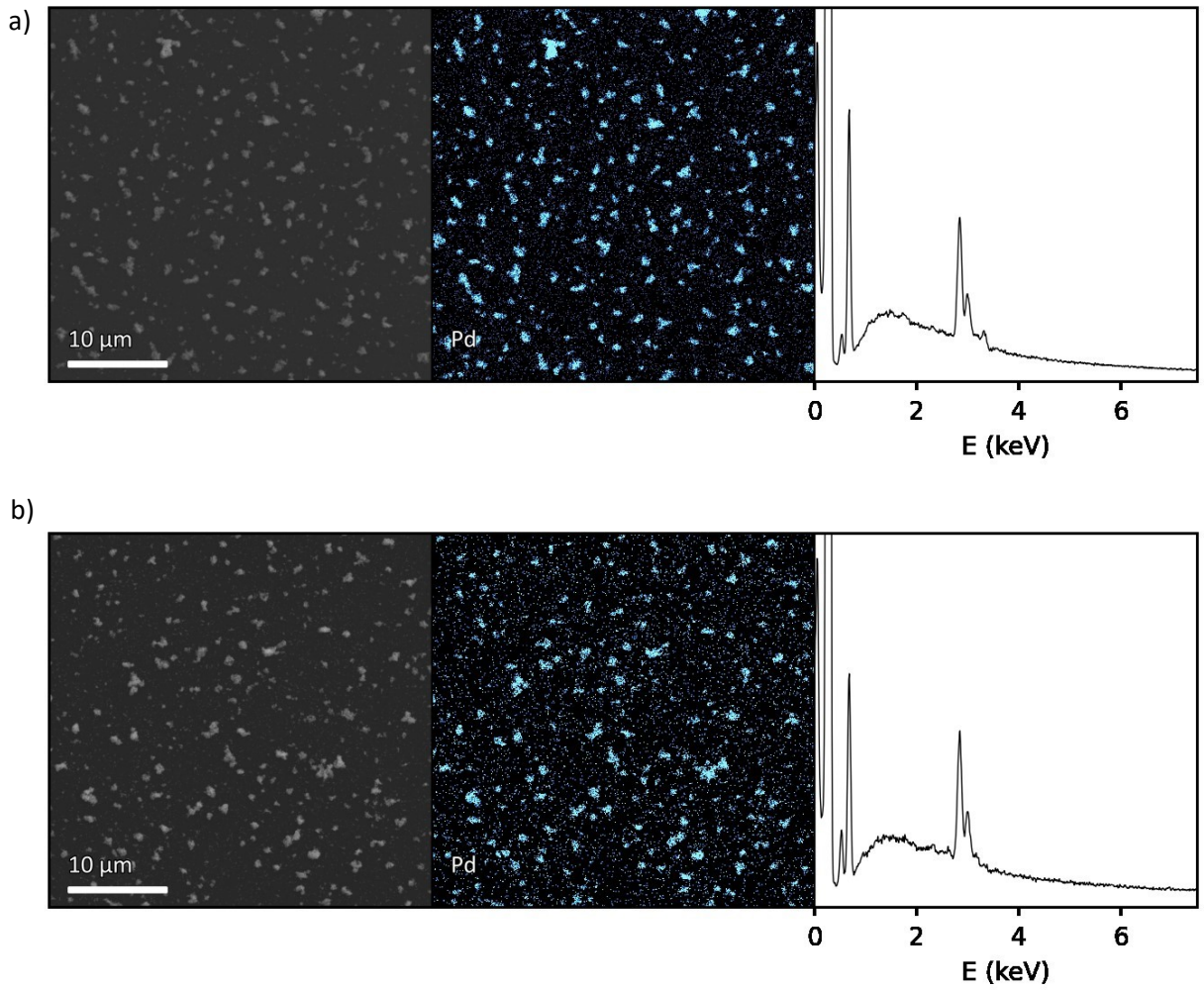

Figure S41. SEM images of Pd thin films a) before and b) after test of stability towards HER. The left images are the SEM image, the middle images are the EDX map of Pd, while the left images are the corresponding EDX spectra.

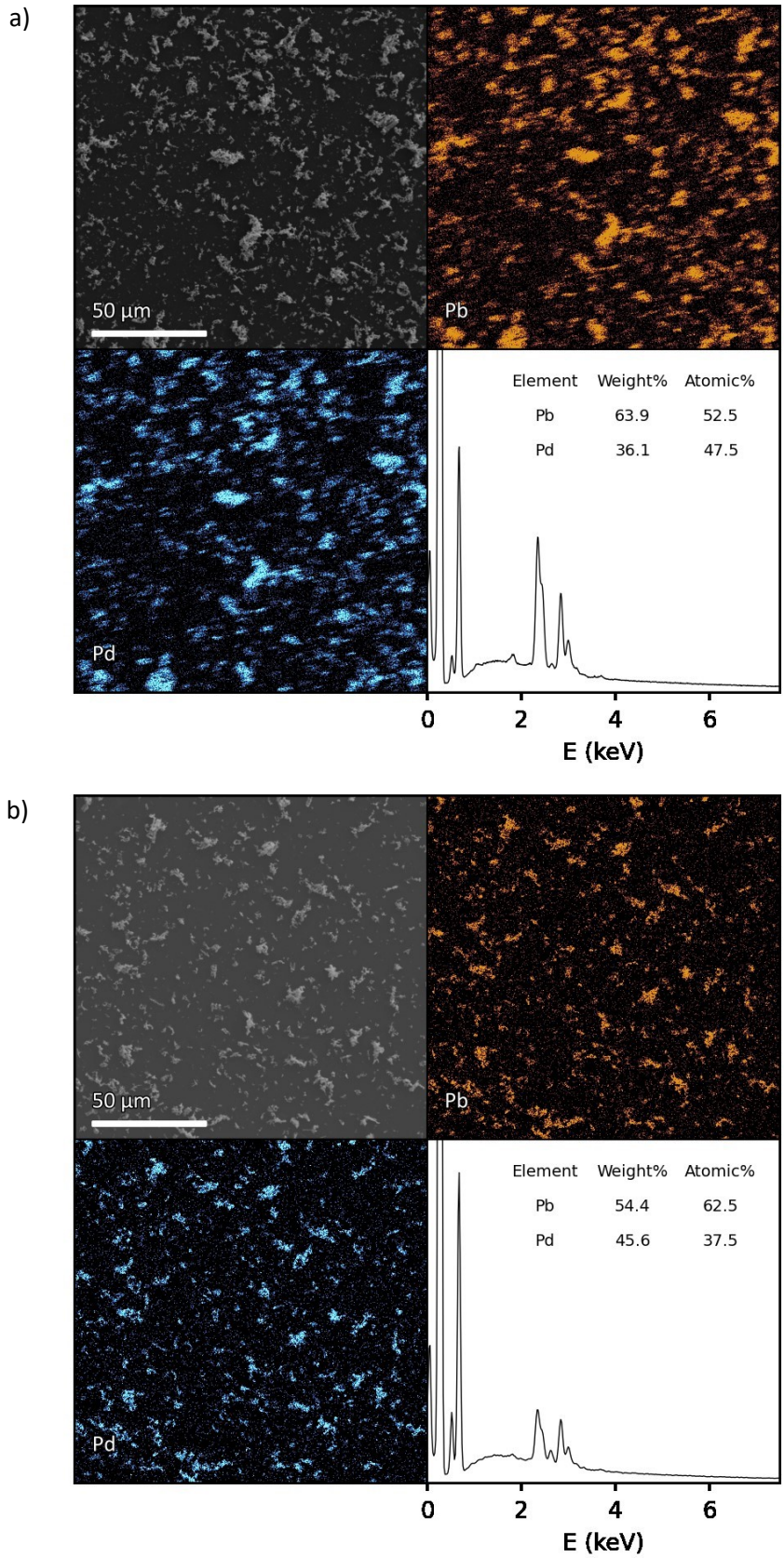

Figure S42. SEM images of Pb_3Pd_5 thin films a) before and b) after test of stability towards HER. The top left images are the SEM image, the top right and lower left images are an EDX map of Pb and Pd respectively, and the lower right images are the corresponding EDX spectra.

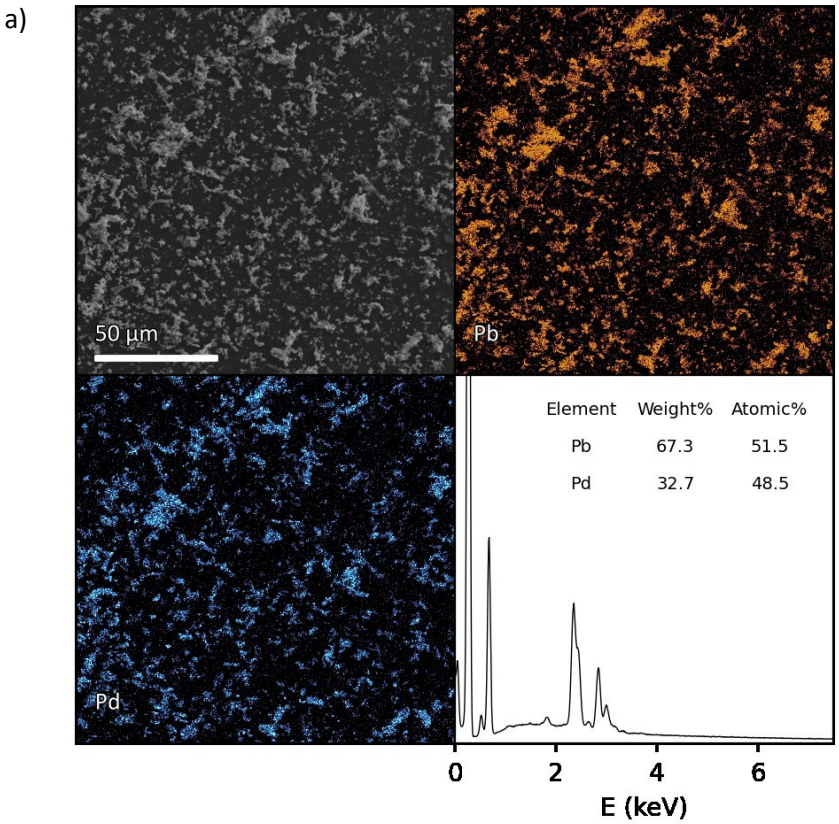

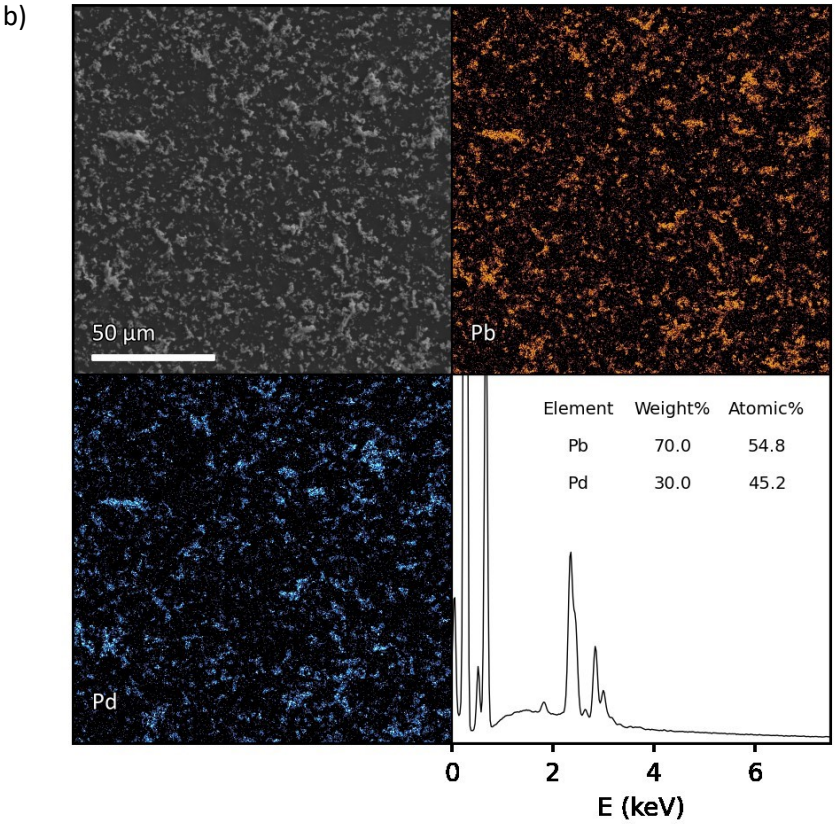

Figure S43. SEM images of Pb_9Pd_{13} thin films a) before and b) after test of stability towards HER. The top left images are the SEM image, the top right and lower left images are the EDX maps of Pb and Pd respectively, and the lower right images are the corresponding EDX spectra.

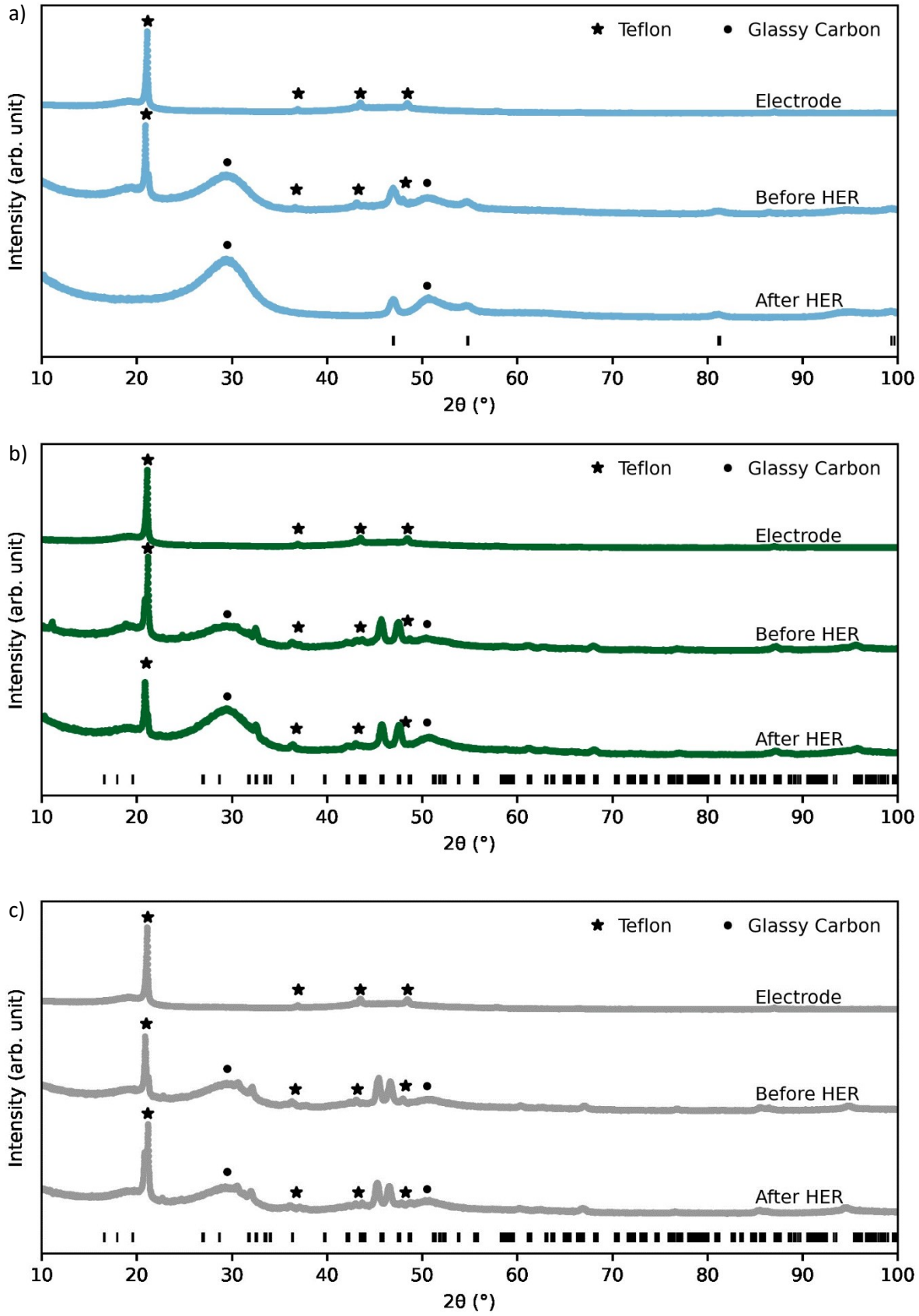

Figure S44. PXRD before and after HER compared with an electrode without a thin film. The black vertical lines indicate the placement of the Bragg peaks. a) Pd, b) Pb_3Pd_5, and c) Pb_9Pd_{13}. Peaks from the Teflon background are marked with a star, while peaks from the glassy carbon are marked with a dot.

References:

1. K. Momma and F. Izumi, *J. Appl. Crystallogr.*, 2011, **44**, 1272-1276.
2. M. Ellner, T. Gödecke and K. Schubert, *Int. J. Mater. Res.*, 1973, **64**, 566-568.
3. X. Yang, P. Juhás, C. L. Farrow and S. J. L. Billinge, *arXiv: Materials Science*, 2014.
4. O. Loebich and C. J. Raub, *J. less-common met.*, 1977, **55**, 67-76.
5. H. W. Mayer, M. Ellner and K. Schubert, *J. less-common met.*, 1980, **71**, P29-P38.
6. H. W. Mayer and K. Schubert, *J. less-common met.*, 1980, **72**, P1-P10.
7. E. E. Havinga, H. Damsma and P. Hokkeling, *J. less-common met.*, 1972, **27**, 169-186